Ⅳ　研究成果の刊行物・別冊

JOURNAL OF BACTERIOLOGY, Feb. 2007, p. 1099–1108 Vol. 189, No. 3
0021-9193/07/$08.00+0 doi:10.1128/JB.01471-06

Structural Characterization of a Specific Glycopeptidolipid Containing a Novel *N*-Acyl-Deoxy Sugar from *Mycobacterium intracellulare* Serotype 7 and Genetic Analysis of Its Glycosylation Pathway▽†

Nagatoshi Fujiwara,[1]* Noboru Nakata,[2] Shinji Maeda,[1,3] Takashi Naka,[1,4] Matsumi Doe,[5] Ikuya Yano,[4] and Kazuo Kobayashi[1]‡

Department of Host Defense, Osaka City University Graduate School of Medicine, Osaka,[1] Department of Microbiology, Leprosy Research Center, National Institute of Infectious Diseases, Tokyo,[2] Molecular Epidemiology Division, Mycobacterium Reference Center, The Research Institute of Tuberculosis, Japan Anti-Tuberculosis Association, Tokyo,[3] Japan BCG Central Laboratory, Tokyo,[4] and Department of Chemistry, Graduate School of Science, Osaka City University, Osaka,[5] Japan

Received 18 September 2006/Accepted 13 November 2006

The nontuberculous *Mycobacterium avium-Mycobacterium intracellulare* complex (MAC) is distributed ubiquitously in the environment and is an important cause of respiratory and lymphatic disease in humans and animals. These species produce polar glycopeptidolipids (GPLs), and of particular interest is their serotype-specific antigenicity. Structurally, GPLs contain an *N*-acylated tetrapeptide-amino alcohol core that is glycosylated at the C terminal with 3,4-di-*O*-methyl rhamnose and at the D-*allo*-threonine with a 6-deoxy-talose. This serotype nonspecific GPL is found in all MAC species. The serotype-specific GPLs are further glycosylated with a variable haptenic oligosaccharide at 6-deoxy-talose. At present, 31 distinct serotype-specific GPLs have been identified on the basis of oligosaccharide composition, and the complete structures of 14 serotype-specific GPLs have been defined. It is considered that the modification of the GPL structure plays an important role in bacterial physiology, pathogenesis, and host immune responses. In this study, we defined the complete structure of a novel serotype 7 GPL that has a unique terminal amido sugar. The main molecular mass is 1,874, and attached to the tetrapeptide-amino alcohol core is the serotype 7-specific oligosaccharide unit of 4-2′-hydroxypropanoyl-amido-4,6-dideoxy-2-*O*-methyl-β-hexose-(1→3)-α-L-rhamnose-(1→3)-α-L-rhamnose-(1→3)-α-L-rhamnose-(1→2)-α-L-6-deoxy-talose. Moreover, we isolated and characterized the serotype 7-specific gene cluster involved in glycosylation of the oligosaccharide. Nine open reading frames (ORFs) were observed in the cluster. Based on the sequence homology, the ORFs are thought to participate in the biosynthesis of the serotype 7 GPL.

About 10% of mycobacterial diseases are caused by nontuberculous mycobacteria. Among them, the closely related *Mycobacterium avium* and *Mycobacterium intracellulare* are commonly grouped as *M. avium-intracellulare* complex (MAC). Organisms of this complex are ubiquitous in nature and have been isolated from water, soil, plants, house dust, and other environmental sources. MAC infections have become increasingly common, and MAC is the most common cause of disease due to nontuberculous mycobacteria in humans (13). These organisms have distinctive laboratory characteristics, are not communicable from person to person, and are often resistant to standard antituberculosis drugs.

The mycobacterial cell wall contains numerous antigenic or immunoregulatory glycolipid molecules with great structural diversity that are considered to be involved in the bacterial virulence through host immune responses (6, 19, 31, 33). The polar glycopeptidolipids (GPLs) produced by MAC species are of particular interest because of their serotype-specific antigenicity (9). To better understand the mechanisms of pathogenesis and drug resistance of MAC, it is necessary to elucidate the molecular structure and biochemical characteristics of the lipid components.

Structurally, GPLs contain a tetrapeptide-amino alcohol core, D-phenylalanine-D-*allo*-threonine-D-alanine-L-alaninol (D-Phe-D-*allo*-Thr-D-Ala-L-alaninol), with an amido-linked 3-hydroxy or 3-methoxy C26-C34 fatty acid at the N-terminal of D-Phe (5). The D-*allo*-Thr and terminal L-alaninol are further linked with 6-deoxy-talose (6-d-Tal) and 3,4-di-*O*-methyl-rhamnose (3,4-di-*O*-Me-Rha), respectively. This core GPL is found in all species of MAC and shows a common antigenicity (1). The serotype-specific GPLs are further glycosylated with a variable haptenic oligosaccharide at 6-deoxy-talose. At present, 31 distinct serotype-specific polar GPLs have been identified biochemically, and the complete structure of GPLs is partly defined by the serotype 1 to 4, 8, 9, 12, 14, 17, 19 to 21, 25, and 26 GPLs (9). The standard technique for classification of MAC strains has been serologic typing based on the oligosaccharide (OSE) residue of the GPL. More recently, advanced chemical synthesis of various haptenic OSEs was demonstrated, and the genes encoding the glycosylation pathways in

* Corresponding author. Mailing address: Department of Host Defense, Osaka City University Graduate School of Medicine, 1-4-3 Asahi-machi, Abeno-ku, Osaka 545-8585, Japan. Phone: 81 (6) 6645 3746. Fax: 81 (6) 6645 3747. E-mail: fujiwara@med.osaka-cu.ac.jp.

‡ Present address: Department of Immunology, National Institute of Infectious Diseases, Tokyo, Japan.

† Supplemental material for this article may be found at http://jb.asm.org/.

▽ Published ahead of print on 22 November 2006.

biosynthesis of GPL were identified and characterized (10, 17, 26).

We have established a rapid method for serodiagnosis of MAC disease using the GPL and GPL core antigens of MAC and have also shown that the levels of GPL and GPL core antibodies reflect disease activity (12, 14, 22, 23). Otherwise, it has been reported that serotype-specific GPLs participate in the pathogenesis and immunomodulation in the host (2, 18). It is reasonable to hypothesize that modification of the GPL structure plays an important role not only in antigenicity but also in host immune responses and bacterial physiology. In this study, we explored the complete OSE structure of serotype 7 GPL, which has a unique terminal amido sugar and is characterized by a serotype 7-specific gene cluster involved in the glycosylation of the OSE, using the cosmid library technique.

MATERIALS AND METHODS

Bacterial strain and preparation of GPL. *M. intracellulare* serotype 7 strain (ATCC 35847) was purchased from the American Type Culture Collection (Manassa, VA). Two clinical strains (NF 111 and NF 112) of *M. intracellulare* serotype 7 were isolated and kindly provided by Ryoji Maekura (National Hospital Organization, Toneyama National Hospital, Osaka, Japan). GPL was prepared as described previously (20, 22). Briefly, the ATCC 35847 strain of *M. intracellulare* serotype 7 was grown in Middlebrook 7H9 broth (Difco Laboratories, Detroit, MI) with 0.5% glycerol and 10% Middlebrook oleic acid-albumin-dextrose-catalase enrichment (Difco Laboratories) at 37°C for 2 to 3 weeks. Heat-killed bacteria were collected by centrifugation at 2,400 × *g* for 15 min, sonicated, and extracted with chloroform-methanol (2:1, vol/vol). The extractable lipids were dried and hydrolyzed with 0.2 N sodium hydroxide in methanol at 37°C for 2 h. The alkaline-stable lipids were dissolved in chloroform-methanol (2:1, vol/vol). GPL was purified by preparative thin-layer chromatography (TLC) of silicagel G (Uniplate; 20 × 20 cm, 250 μm; Analtech, Inc., Newark, DE). The TLC plate was repeatedly developed with chloroform-methanol-water (65:25:4 and 60:16:2, vol/vol/vol) until a single spot was obtained. To reveal the GPL band, the TLC plate was exposed to iodine vapor after development. The GPL band was marked, and then the silicagels were scraped to elute the GPL with chloroform-methanol (2:1, vol/vol) through a small glass column.

Preparation of OSE moiety. The OSE moiety elongated from D-*allo*-Thr was released from GPL by alkaline borohydride reductive β-elimination (7, 20). GPL was dissolved in ethanol with 5 mg/ml sodium borohydride and 0.5 M sodium hydroxide, followed by stirring at 60°C for 16 h. The reaction mixture was decationized with Dowex 50WX8 beads (Dow Chemical Company, Midland, MI) and centrifuged at 2,400 × *g* for 15 min. The supernatant was collected and coevaporated with 10% acetic acid in methanol under nitrogen to remove the boric acid. The dried residue was partitioned in two layers in chloroform-methanol (2:1, vol/vol) and water. The upper aqueous phase was recovered and evaporated. In these processes, the serotype 7-specific OSE was purified as an oligoglycosyl alditol.

Derivatization of perdeuteromethylated and perdeuteroacetylated OSE. Perdeuteromethylation was conducted by the modified procedure of Hakomori (16). The dried OSE was dissolved in a mixture of dimethyl sulfoxide (1 ml) and sodium hydroxide (1 mg), and 1 ml of deuteromethyl iodide was added. The reaction mixture was stirred at room temperature for 15 min, followed by the addition of 1 ml of water and 1 ml of chloroform. After centrifugation at 2,400 × *g* for 15 min, the upper water layer was discarded. The chloroform layer was washed repeatedly with water to remove any water-soluble components and then evaporated to dryness. Perdeuteroacetylation of OSE was performed by reacting OSE with pyridine-deuteroacetic anhydride (1:1, vol/vol) for 16 h, and the product was dried completely to remove the pyridine.

FAB/MS analysis of intact GPL and OSE. The molecular weight was determined by fast atom bombardment-mass spectrometry (FAB/MS) with a JMS SX102A double-focusing mass spectrometer (JEOL, Tokyo, Japan). The target gas was xenon, and the accelerating voltage was 8 kV. Intact GPL was analyzed by FAB/MS in both positive and negative ion mode with *m*-nitro-benzyl alcohol as the matrix. The perdeuteroacetylated derivative of OSE was analyzed by FAB/MS in positive ion mode with *m*-nitro-benzyl alcohol as the matrix.

GC and GC/MS analyses of OSE. To determine the glycosyl composition and linkage position, gas chromatography (GC) and GC/MS analyses of partially methylated alditol acetate derivatives were performed. Partially deuteromethylated alditol acetates were prepared from perdeuteromethylated OSE by hydrolysis with 2 N trifluoroacetic acid at 120°C for 2 h, reduction with 10 mg/ml sodium borodeuteride at 25°C for 2 h, and acetylation with acetic anhydride at 100°C for 1 h (8, 21). GC was performed using a 5890 series II gas chromatograph (Hewlett Packard, Avondale, PA) equipped with the fused capillary column SPB-1 (30 m, 0.25-mm inside diameter; Supelco, Inc., Bellefonte, PA). Helium was used for electron impact (EI)/MS and *iso*-butane was used for chemical ionization (CI)/MS as the carrier gas. The JMS SX102A double-focusing mass spectrometer was connected to GC as the mass detector. The molecular separator and the ion source energy were 70 eV for EI and 30 eV for CI, and the accelerating voltage was 8 kV. The DL configurations of Rha residues were determined by comparative GC/MS analysis of trimethylsilylated (*R*)-(−)-2-butyl glycosides and (*S*)-(+)-2-butyl glycosides prepared from an authentic L-Rha standard (15).

NMR analysis of OSE. The GPL was deuterium dissolved in chloroform-d ($CDCl_3$)/methanol-d_4 (CD_3OD) (2:1, vol/vol). To define the anomeric configurations of each glycosyl residue, ^1H and ^{13}C nuclear magnetic resonance (NMR) was employed. Both homonuclear correlation spectrometry, and ^1H-detected [^1H, ^{13}C] heteronuclear multiple-quantum correlation (HMQC) were recorded with a Bruker AVANCE-600 spectrometer (Brucker BioSpin K.K., Osaka, Japan), as described previously (9, 20, 27).

Construction of the *M. intracellulare* cosmid library. Genomic DNA of *M. intracellulare* serotype 7 strain ATCC 35847 was prepared by mechanical disruption of bacterial cells, which was accomplished by homogenizing a bacterial pellet with glass beads in phosphate-buffered saline, followed by phenol-chloroform extraction and precipitation with ethanol. Genomic DNA fragments randomly sheared to 30- to 50-kb fragments during the extraction process were fractionated and electroeluted from agarose gels using a Recochip (Takara, Bio, Inc., Kyoto, Japan). These DNA fragments were rendered blunt-ended using T4 DNA polymerase and deoxynucleoside triphosphates, followed by ligation to dephosphorylated arms of pYUB412 (XbaI-EcoRV and EcoRV-XbaI), which was kindly given by William R. Jacobs, Jr. (Department of Microbiology and Immunology, Albert Einstein College of Medicine, New York, NY). After in vitro packaging using Gigapack III Gold extracts (Stratagene, La Jolla, CA), recombinant cosmids were introduced into the *Escherichia coli* STBL2 [F⁻ *mcrA* Δ(*mcrBC-hsdRMS-mrr*) *endA1 recA1 lon gyrA96 thi supE44 relA1* λ⁻ Δ(*lac-proAB*)] and stored at −80°C in 50% glycerol.

Isolation of cosmid clones carrying the *rtfA* gene and sequence analysis. PCR was used to isolate cosmid clones carrying the rhamnosyltransferase (*rtfA*) gene with primers *rtfA*-F (5′-TTTTGGAGCGACGAGTTCATC-3′) and *rtfA*-R (5′-GTGTAGTTGACCACGCCGAC-3′). *rtfA* encodes an enzyme responsible for the transfer of Rha to 6-d-Tal in OSE (11, 26). The insert of cosmid clone 49 was sequenced using a BigDye Terminator, version 3.1, Cycle Sequencing Kit (Applied Biosystems, Foster City, CA) and an ABI Prism 310 gene analyzer (Applied Biosystems). The putative function of each open reading frame (ORF) was identified by similarity searches between the deduced amino acid sequences and known proteins using BLAST (http://www.ncbi.nlm.nih.gov/BLAST/) and FramePlot (http://www.nih.go.jp/~jun/cgi-bin/frameplot.pl) with the DNASIS computer program (Hitachi Software Engineering, Yokohama, Japan). To confirm the presence of ORFs in clinical strains of *M. intracellulare* serotype 7, PCRs were performed by using the primers of each ORF (Table 1).

Nucleotide sequence accession number. The nucleotide sequence reported here has been deposited in the NCBI GenBank database under accession number AB274811.

RESULTS

Purification and molecular weight of intact GPL. Serotype 7 GPL of *M. intracellulare* was purified repeatedly by silica gel TLC and showed as a single spot on the TLC plate (Fig. 1A). The R_f values of serotype 7 GPL were 0.42 and 0.24 on TLC with the developing solvents (chloroform-methanol-water at 65:25:4 and 60:16:2, vol/vol/vol, respectively). The main pseudomolecular ions of positive and negative FAB/MS were *m/z* 1897 for $[M+Na]^+$ and *m/z* 1873 for $[M-H]^-$ (Fig. 1B). These results showed that the main molecular weight of serotype 7 GPL was 1874 and differed from the molecular weights of other GPLs (9, 25), implying that it has a novel carbohydrate chain elongated from D-*allo*-Thr.

TABLE 1. Sequences of primers used for amplifying ORFs in this study

ORF	Forward sequence (5′–3′)	Reverse sequence (5′–3′)
ORF 1	GTGAAATTTGCCCTGG CGAG	TCAGCCAAAGCGCCT CGTGT
ORF 2	GTGGTATTGAATACAC GCAT	TCAAACCTCCGCCGA TTTCG
ORF 3	GTGCCCGAAGTTCCTT CCGA	TCAACGGGTGCGGTG TCGCG
ORF 4	ATGCCTGCTGAGATCC CGTT	CTATGTGCTCACTTTC TTAA
ORF 5	TTGGCAGCCTGGAGCG ACCG	TCACAGTTGCGTTCC GTCAC
ORF 6	GTGACGCGCCTTGACA CGGG	TCATGCGATTGCGCC CTGTT
ORF 7	GTGGCAATTCGCGCCG CGCC	TCACCCAAACTTGCG GCCCT
ORF 8	GTGGCGTTGGGCGCCC CTAG	TCAGCCGCTGATAAA CGCTC
ORF 9	ATGAGCGAGCCGGCTG GCCG	CTATTGGGACGGACC CCTGA

Glycosyl composition of OSE. To determine the glycosyl composition of OSE, alditol acetate derivatives from serotype 7 GPL were analyzed by GC and GC/MS. The structurally defined serotype 4 GPL was used as a reference standard (9, 28). From the comparison of the retention time and spectra on GC and GC/MS (Fig. 2), the alditol acetate derivatives of serotype 7 GPL showed the presence of 3,4-di-*O*-Me-Rha, Rha, 6-d-Tal, and an unknown sugar residue (X1) in a ratio of approximately 1:3:1:1. The alditol acetate of X1 was eluted with a retention time (22.9 min) greater than that of glucitol acetate on SPB-1 columns. The CI/MS spectrum of X1 showed $[M+H]^+$ at *m/z* 420 as a parent ion and *m/z* 360 as a loss of 60 (acetate). The fragment ions of X1 sugar showed characteristic patterns in EI/MS. *m/z* 332 and 87 indicated the cleavage of C-4–C-5, and *m/z* 290, 272, 230, and 170 were fragmented as a loss of 42 (ketene) or 60 (acetate). Similarly, *m/z* 302 and 117 indicated the cleavage of C-2–C-3, and *m/z* 200 was fragmented as a loss of 42 and 60 (Fig. 3). These results indicated that X1 was 4,6-dideoxy-hexose (Hex). The molecular weight, 419, of X1 and fragment ions 115 and 87 were consistent with the presence of one amido group attached to 2′-hydroxypropanoic acid. Taken together, X1 was structurally determined to be 4-2′-hydroxypropanoyl-amido-4,6-dideoxy-2-*O*-methyl-Hex.

Linkage and sequence analyses of OSE. To determine the glycosyl linkage and sequence of OSE, GC/MS of perdeuteromethylated alditol acetates and FAB/MS of deuteroacetylated oligoglycosyl alditol from serotype 7 OSE were performed. The EI/MS spectra of perdeuteromethylated alditol acetates (Fig. 4) were assigned to the three major peaks, 1,3,4,5-tetra-*O*-deuteromethyl-2-*O*-acetyl-6-deoxytalitol (*m/z* 109, 132, 154, 167, and 214), 2,4-di-*O*-deuteromethyl-1,3,5-tri-*O*-acetyl-rhamnitol (*m/z* 121, 134, 205, 240, and 253), and 3-*O*-deuteromethyl-1,5-di-*O*-acetyl-4-2′-*O*-deuteromethyl-propanoyl-deuteromethylamido-4,6-dideoxy-2-*O*-methyl-hexitol (*m/z* 87, 105, 165, 222, and 300). These results demonstrated that the 6-d-Tal residue was linked at C-2, Rha was linked at C-1 and C-3, and the nonreducing terminus, 4-2′-hydroxypropanoyl-amido-4,6-dideoxy-2-*O*-methyl-Hex, was 1-linked. The FAB/MS spectrum of deuteroacetylated oligoglycosyl alditol from serotype 7 OSE afforded the expected molecular ions $[M+Na]^+$ and $[M+H]^+$ at *m/z* 1398 and 1376, respectively, together with the characteristic mass increments in the series of glycosyloxonium ions formed on fragmentation at *m/z* 322, 558, 794, and 1030 (Fig. 5). The fragment ion, *m/z* 322, was in accord with a 4-2′-*O*-deuteroacetyl-propanoyl-amido-4,6-dideoxy-2-*O*-methyl-3-*O*-deuteroacetyl-hexosyl residue at the nonalditol terminus. In addition, each fragment and parent ion (*m/z* 558, 794, 1030, and 1376) showed three additional molecular

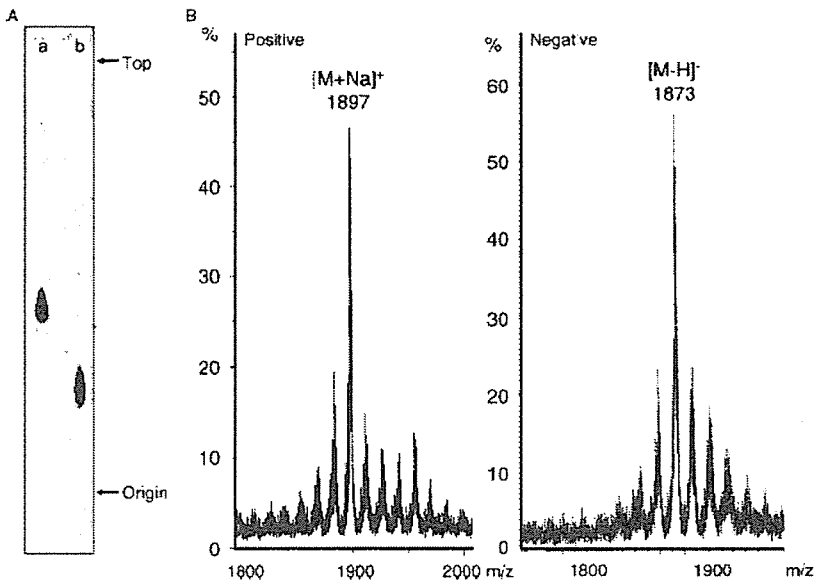

FIG. 1. TLC patterns (A) and FAB/MS spectra (B) of intact serotype 7 GPL derived from *M. intracellulare* strain ATCC 35847. The TLC solvent systems were chloroform-methanol-water (a, 65:25:4; b, 60:16:2, by volume). The TLC plate was sprayed with 10% sulfuric acid in ethanol and was charred at 180°C for 5 min. The FAB/MS spectra were acquired using an *m*-nitro-benzyl alcohol matrix, and the pseudomolecular ions were detected as $[M+Na]^+$ in positive mode and $[M-H]^-$ in negative mode.

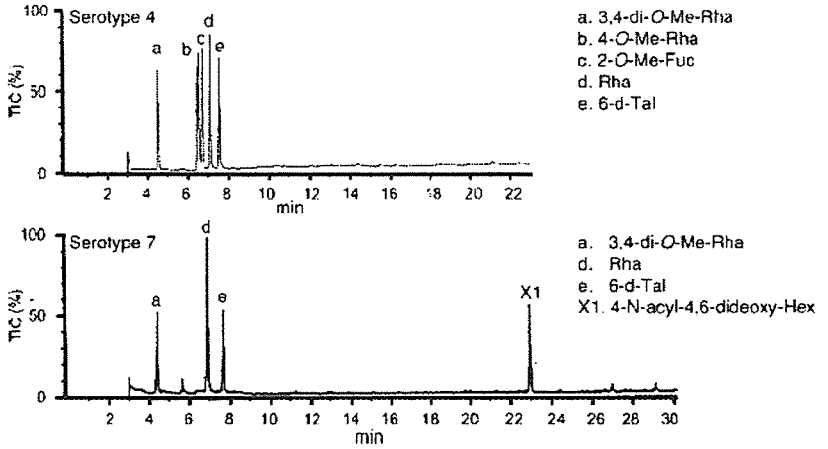

FIG. 2. GC spectra of the alditol acetate derivatives from serotype 4 and 7 GPLs. Total ion chromatograms are shown. GC was conducted on an SPB-1 fused silica column with a temperature program of 160°C for 2 min, followed by a rise of 4°C/min to 220°C and then maintained at 220°C for 13 min.

Rha and 6-d-Tal residues. Rha residues were determined to be in the L absolute configuration by comparative GC/MS analysis of trimethylsilylated (*R*)-(−)-2-butyl glycosides and (*S*)-(+)-2-butyl glycosides (see Fig. S1 in the supplemental material). Taken together, these results established the sequence and linkage arrangement: 4-2′-hydroxypropanoyl-amido-4,6-dideoxy-2-*O*-methyl-Hex-(1→3)-L-Rha-(1→3)-L-Rha-(1→3)-L-Rha-(1→2)-L-6-d-Tal, exclusively.

NMR analysis of serotype 7 OSE. The ^{1}H NMR and ^{1}H-^{1}H correlation spectrometry analyses of GPL revealed six distinct anomeric protons with corresponding H1-H2 cross-peaks in the low field region at δ5.01, 4.98, 4.96, 4.88, 4.69 (J_{1-2} 2–3 Hz, indicative of α-anomers), and 4.55 (a doublet, J_{1-2} 7.8 Hz, indicative of a β-hexosyl unit). When further analyzed by ^{1}H-detected [^{1}H-^{13}C] two-dimensional HMQC, the anomeric protons resonating at δ5.01, 4.98, 4.96, 4.88, 4.69, and 4.55 have C-1s resonating at δ101.66, 101.17, 95.80, 102.40, 99.87, and 103.21, respectively. The J_{CH} values for each of these protons were calculated to be 171, 169, 171, 175, 171, and 159 Hz by the measurement of the inverse-detection nondecoupled two-dimensional HMQC shown in Fig. 6. These results are summarized (see Table S1 in the supplemental material), and establish that the terminal amido-Hex was a β configuration and the others were α-anomers.

Cloning and sequence of the serotype 7 GPL biosynthesis cluster. To isolate the serotype 7 GPL biosynthesis cluster, the genomic cosmid library of an *M. intracellulare* serotype 7 strain, ATCC 35847, was constructed. Primers were designed for amplification of a region corresponding to the *rftA* gene. DNA was extracted from each clone by boiling. By using colony PCR with *rftA* primers, more than 100 cosmid clones were tested, and the positive clone 49 was isolated from the *E. coli* transductants. The

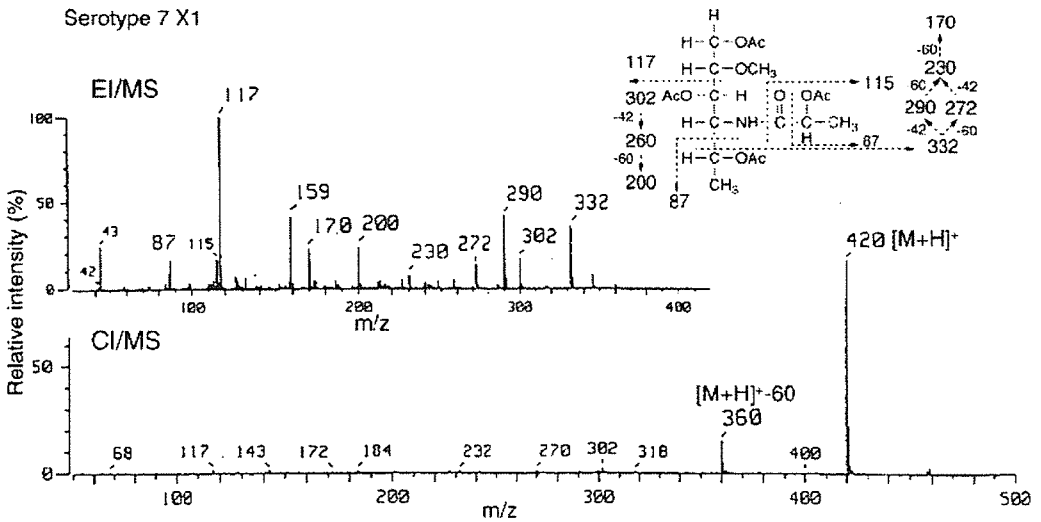

FIG. 3. EI/MS and CI/MS spectra of the alditol acetate derivative from X1. The patterns of prominent fragment ions are illustrated. The alditol acetate derivative was resolved on an SPB-1 fused silica column with a temperature program of 160°C for 2 min, followed by a rise of 4°C/min to 220°C and then maintained at 220°C for 13 min.

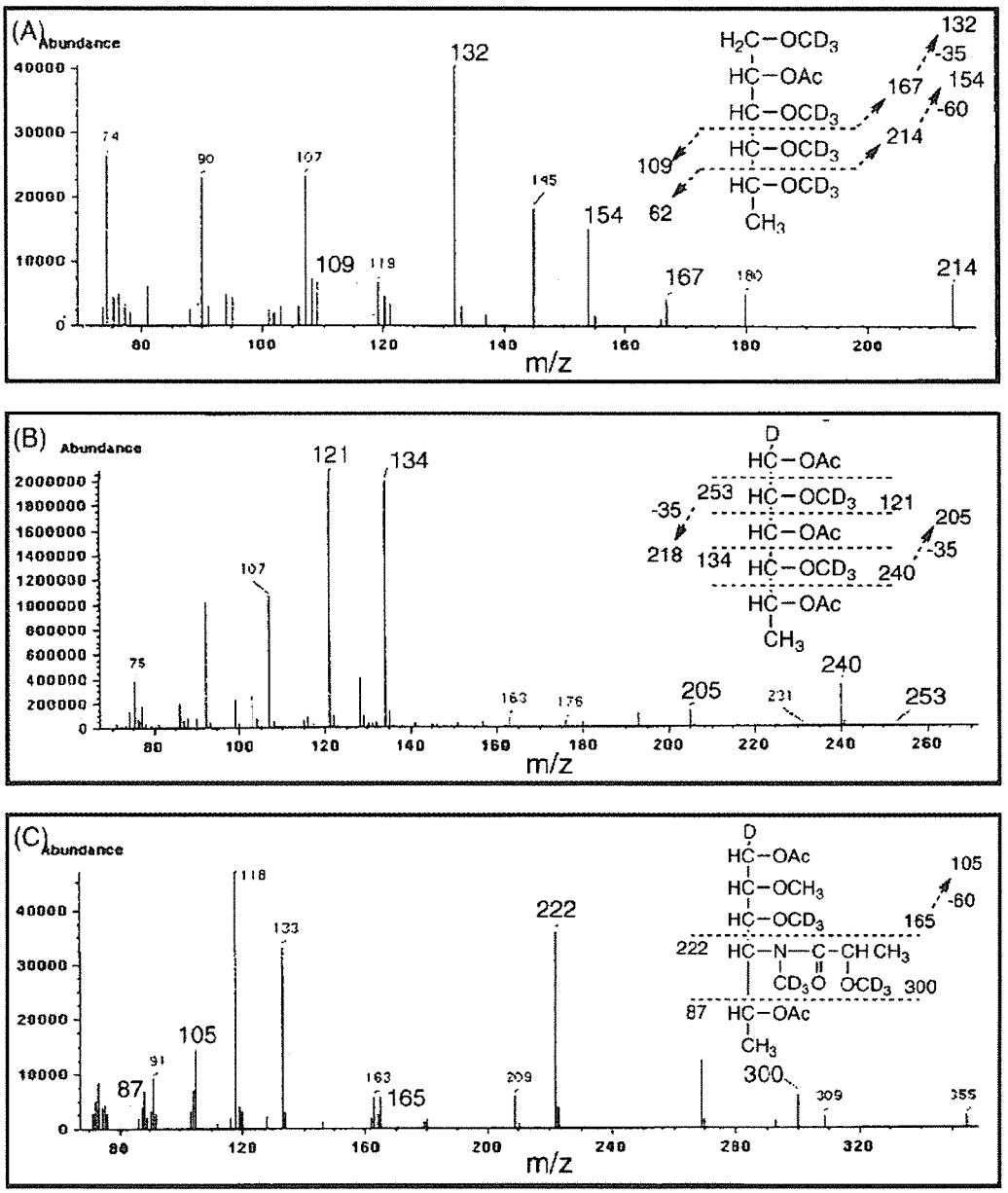

FIG. 4. EI/MS spectra of individual perdeuteromethylated alditol acetate derivative derived from serotype 7 OSE. The formation of prominent fragment ions is illustrated, and they were assigned to 1,3,4,5-tetra-*O*-deuteromethyl-2-*O*-acetyl-6-deoxytalitol (A), 2,4-di-*O*-deuteromethyl-1,3,5-tri-*O*-acetyl-rhamnitol (B), and 3-*O*-deuteromethyl-1,5-di-*O*-acetyl-4-2'-*O*-deuteromethyl-propanoyl-deuteromethyl-amido-4,6-dideoxy-2-*O*-methyl-hexitol (C).

38.4-kb insert of cosmid clone 49 was sequenced. The 19.7-kb region in this clone was deposited in the NCBI GenBank database (accession no. AB274811). The *rtfA* gene in cosmid clone 49 from *M. intracellulare* serotype 7 had 98.4% DNA identity with *M. intracellulare* strain 5509-Borstel (serotype 13) and around 84% DNA identity with *M. avium* strains. The understanding of gene function was based on the comparison of this sequence information to homologous regions in the genome sequence data from *M. avium* strain A5 (serotype 4, NCBI GenBank AY130970) (24). The gene order from *mtfB* (encoding methyltransferase) to *gtfB* (encoding glycosyltransferase) including *rtfA* was identical to that of the *M. avium* strain A5 cluster (Fig. 7A). The DNA region between ORF 1 and ORF 9 (11.0 kb) was unique to *M. intracellulare* serotype 7 strain ATCC 35847, and nine ORFs were observed. In this region, the insertion of IS elements and transposons was not detected. To confirm that the region of ORF 1 to ORF 9 is specific to *M. intracellulare* serotype 7, we showed the presence of the nine novel ORFs in two clinical isolates of *M. intracellulare* serotype 7 by PCR using the nine ORFs as primers. All ORFs in the ATCC 35847 strain were conserved in the clinical serotype 7 strains, although ORF 6 in the NF 112 strain was detected with a band about 1.3 kb longer (Fig. 7B). Sequence

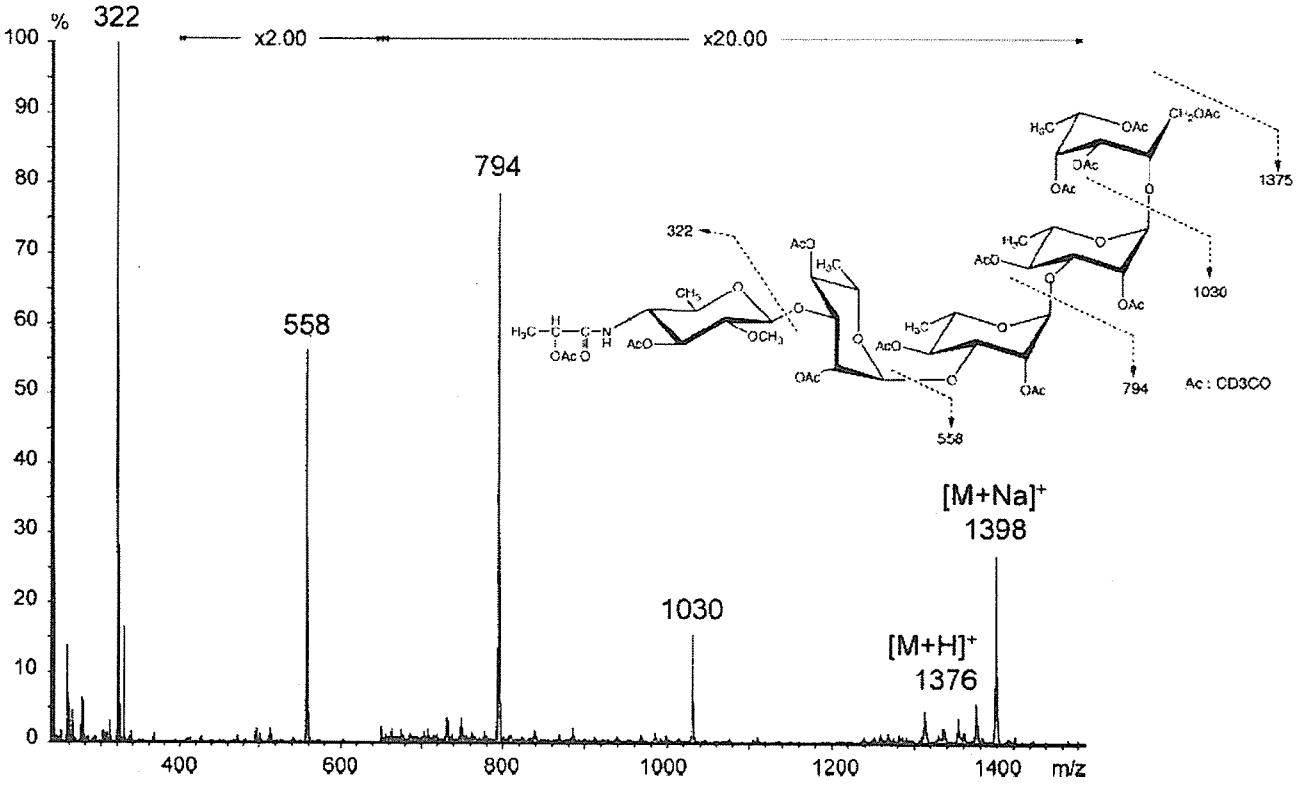

FIG. 5. FAB/MS spectrum of the deuteroacetylated derivative of serotype 7 OSE. The formation of the characteristic increment of fragmentation ions is illustrated. The matrix was *m*-nitro-benzyl alcohol.

analysis of the ORF 6 region in the NF 112 strain showed the insertion of a transposon. Almost none of the ORFs of serotype 7 strains were detected in the reference strains of serotypes 2, 4, 8, 12, 16, and 17, although the PCR bands of some ORFs were positive in other serotype strains. Based on the alignments of genetic maps and comparison to the database provided by NCBI GenBank, these ORFs were homologous to the regions involved in the glycosylation of OSE (Table 2). The deduced amino acid sequence of ORF 1 had much similarity to three putative glycosyltransferases, GtfA, GtfB, and RtfA, of *M. avium* strains. The similarity of the deduced amino acid sequences suggested the possibility that the function of ORF 2 and ORF 3 was to encode methyltransferase and glycosyltransferase Rv1516c (GtfTB). Moreover, from the similarity of the deduced amino acid sequences, ORFs 4, 8, and 9 seem to be aminotransferase, acyltransferase, and glycosyltransferase Rv1518, respectively. Although the homology score was not very high, the deduced amino acid sequences of ORFs 5, 6, and 7 were similar to those for carbamoyl phosphate synthase, nucleotide sugar epimerase, and metallophosphoesterase, respectively. These results suggest that this region of DNA is responsible for the biosynthesis of serotype 7-specific GPL.

DISCUSSION

Nontuberculous mycobacteria, including the pathogenic species belonging to MAC, have serotype-specific GPLs that are important components of the outer layer of the lipid-rich cell walls (6). Structural analyses of some serotype-specific GPLs derived from the predominant clinical isolates have been reported (28), but further structural analyses remain to be performed. The present study describes the chemical structure of the serotype 7 GPL derived from *M. intracellulare*.

We determined the glycosyl composition, linkage positions, and anomeric and ring configurations of glycosyl residues in serotype 7 GPL, which suggested that its OSE is 4-2′-hydroxypropanoyl-amido-4,6-dideoxy-2-*O*-methyl-β-Hex-(1→3)-α-L-Rha-(1→3)-α-L-Rha-(1→3)-α-L-Rha-(1→2)-L-6-d-Tal (Fig. 8). Chatterjee and Khoo have classified the structures of surface GPLs of MAC based on divergent biosynthesis (9). Serotype 7 GPL was assigned to polar GPL group 2 by its chemical structure. Serotype 12, 17, and 19 GPLs have been classified into group 2 GPL, which is commonly composed of *R*→α-L-Rha-(1→3)-α-L-Rha-(1→2)-L-6-d-Tal (*R*, variable region). The external sugar of serotype 7 GPL was a characteristic amido sugar that is composed of 4-2′-hydroxypropanoyl-amido-4,6-dideoxy-2-*O*-methyl-Hex. The presence of an amido sugar has been reported in only four GPLs, serotypes 12, 14, 17, and 25 (8, 9). Bozic et al. demonstrated that the OSE structure of serotype 12 GPL is 4-2′-hydroxypropanoyl-amido-4,6-dideoxy-3-*O*-methyl-β-D-Glu-(1→3)-4-*O*-methyl-α-L-Rha-(1→3)-α-L-Rha-(1→3)-α-L-Rha-(1→2)-α-6-d-Tal (4), which closely resembles the serotype 7 GPL. Comparing the detailed carbohydrate structure of serotype 7 GPL to that of serotype 12 GPL revealed that the acylated-amido group and linkage position-bound terminal sugar were the same, but the position of the *O*-methyl group

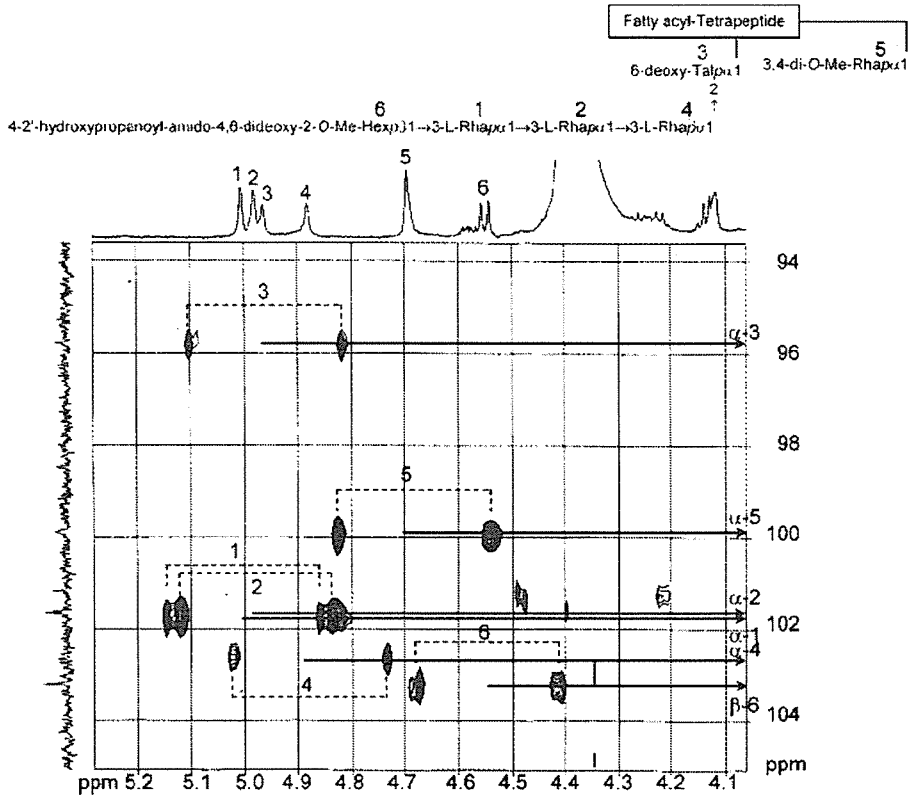

FIG. 6. Nondecoupled ^{1}H-detected [^{1}H-^{13}C] HMQC spectrum of serotype 7 GPL. Cross-peak labels correspond with those shown on the structure.

was different. Moreover, α-L-Rha was next to the terminal Hex in serotype 7 GPL, whereas this position was occupied by 4-*O*-Me-α-L-Rha in serotype 12 GPL. It was difficult to determine the species of acylated-amido sugar because no reference standard was available. In a previous study by Bozic et al., the terminal amido sugar of serotype 12 was assigned as glucose by the proton configuration in ^{1}H-NMR (4). It is possible that the terminal Hex of serotype 7 GPL is a gluco- or galacto-configuration.

Next, we attempted to elucidate the biosynthetic mechanism of GPL by molecular genetics, because very little is known of how the carbohydrate chain elongates in sereotype-specific GPLs. Belisle et al. first identified the *ser2* gene cluster responsible for biosynthesis of OSE in the serotype 2 GPL derived from *M. avium* serotype 2 strain TMC 727, which is mapped to a 22- to 27-kb functional region (3). Krzywinska and Schorey isolated and sequenced a 27.5-kb DNA fragment responsible for the carbohydrate portion of serotype 4 GPL from *M. avium* strain A5 (24). Recently, enzymatic characterization of the glycosyltransferase and methyltransferase in *M. smegmatis*, which can synthesize only nonpolar GPLs, has been reported (29, 30).

As in the serotype-specific polar GPL biosynthesis of MAC, only the *rtfA* gene present in the *ser2* gene cluster was functionally clarified to encode the rhamnosyltransferase responsible for the transfer of L-Rha to 6-d-Tal (11). The precise gene loci correlated to *O*-methylation and glycosylation are poorly understood. In this study, we cloned the serotype 7 GPL biosynthetic cluster and analyzed its sequence. The genetic map of the serotype 7 GPL biosynthetic cluster was compared to that of serotype 4 GPL from *M. avium* strain A5 (24). Although the *mtfB-gtfB* region was fully conserved, significant differences appeared in the neighborhood of this conserved region. Nine novel ORFs were detected only in the serotype 7 strains containing clinical isolates, which strongly suggested that this region is related to the biosynthesis of serotype 7-specific GPL. On the other hand, ORF 6 may not be necessary to serotype 7 GPL biosynthesis because of the insertion of a transposon in a clinical isolate, the NF 112 strain. Based on the analysis of sequence homology (Table 2 and Fig. 7A), the ORFs may be responsible for the glycosylation of serotype 7-specific GPL. From the structural analysis of the serotype 7 GPL and sequence of cosmid clone 49, it is possible to predict the relationship between the biosynthesis of serotype 7 GPL and the function of each ORF (Fig. 8).

rtfA functions to catalyze only the addition of Rha to 6-d-Tal (26), and which gene cluster transfers additional sugars to L-Rha elongated from 6-d-Tal is unclear. ORFs 1, 3, and 9 have high homology to the glycosyltransferases GtfA, Rv1516c, and Rv1518, respectively. We have analyzed similar gene clusters in *M. intracellulare* serotype 12, 16, and 17 strains in addition to the *M. intracellulare* serotype 7 strain. The sequence homology of the region of ORF 1 to ORF 9 was highly conserved between only *M. intracellulare* serotype 7 and 12 strains (unpublished data). ORFs 1, 3, and 9 may lead to transfer of the two

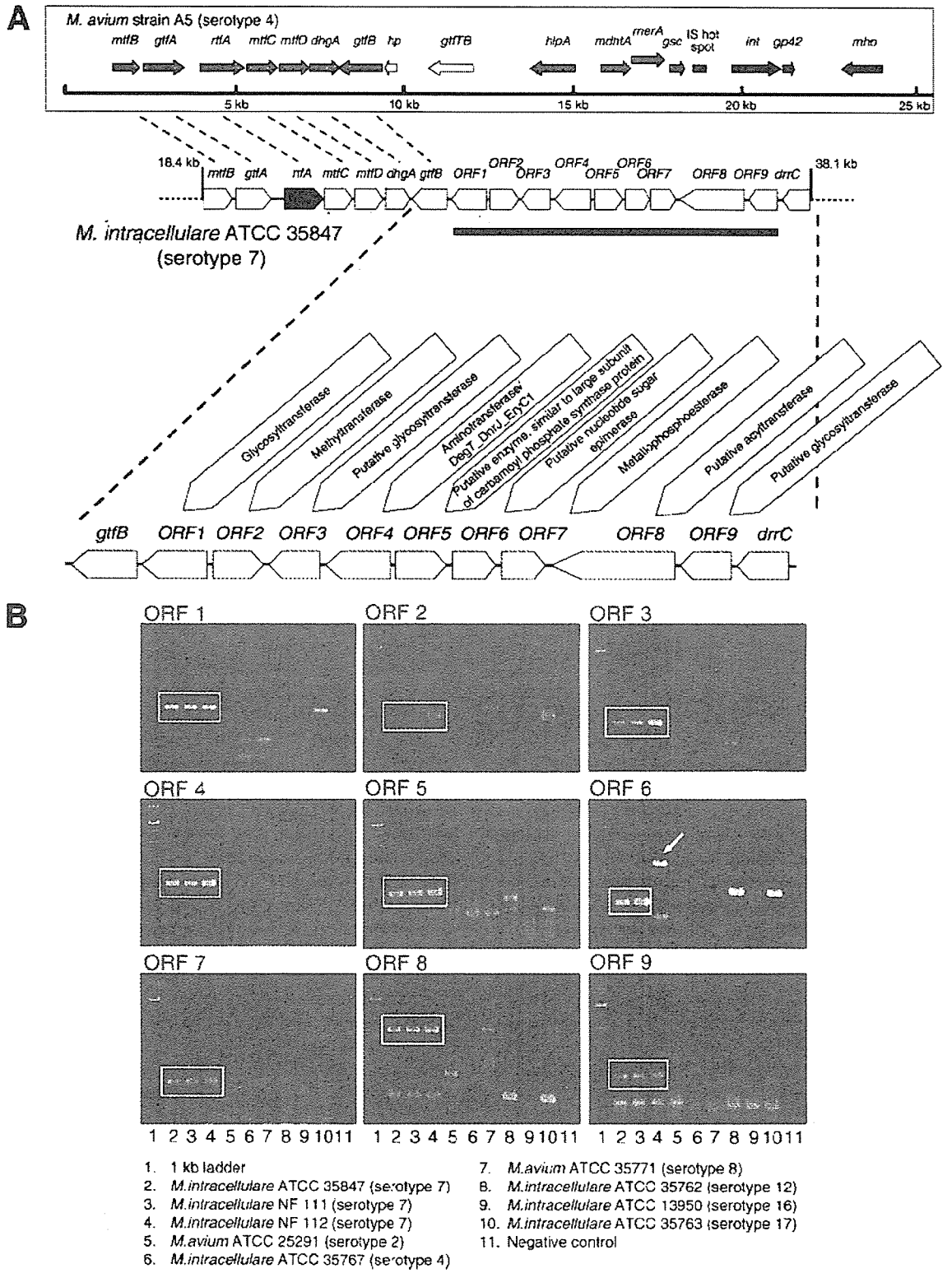

FIG. 7. Genetic map of the GPL biosynthetic cluster and detection of novel serotype 7-specific ORFs. Nine ORFs were observed, and they were homologous to the regions involved in the glycosylation of OSE from the alignment of genetic maps and comparison to the database provided by NCBI GenBank (A). The ORFs in *M. intracellulare* serotype 7 strain ATCC 35847 were serotype 7 specific and preserved in clinical strains (B). The arrow indicates the band of ORF 6 in strain NF 112 that was inserted a transposon. For the genetic map of *M. avium* strain A5 (serotype 4), see the study of Krzywinska and Schorey (24).

TABLE 2. Similarity to protein sequences of ORFs in cosmid clone 49 derived from *M. intracellulare* serotype 7 strain ATCC 35847

ORF	Predicted molecular mass (kDa)	Predicted pI	Similar protein (GenBank accession no.)	E value	Amino acid identity (% matched/total no. of residues)[a]
MtfB	30.5	5.09	Methyltransferase MtfB (Q9WVW3)	E-143	90.4/272
GtfA	46.5	5.84	Glycosyltransferase GtfA (O68999)	0.0	90.7/421
RtfA	46.9	7.76	Rhamnosyltransferase A (Q6U848)	0.0	98.6/419
MtfC	30.0	5.61	Methyltransferase MtfC (Q8GEA1)	E-142	92.1/265
MtfD	32.9	4.89	Methyltransferase MtfD (Q9WW56)	E-147	91.5/272
DhgA	27.3	5.96	Dehydrogenase DhgA (AY130970)	E-120	85.8/260
GtfB	45.5	6.35	Glycosyltransferase GtfB (Q9WW66)	0.0	85.4/419
ORF 1	45.1	6.10	Glycosyltransferase GtfA (O68999)	E-137	58.6/420
ORF 2	30.9	8.14	Methyltransferase (Q885B6)	5E-47	44.3/237
ORF 3	36.6	6.01	Putative glycosyltransferase Rv1516c (P71795)	E-118	66.4/307
ORF 4	40.4	4.92	Aminotransferase/DegT_DnrJ_EryC1 (Q50723)	E-154	75.5/351
ORF 5	36.1	6.43	Putative enzyme, similar to large subunit of carbamoyl phosphate synthase protein (Q92VH3)	1E-39	36.1/321
ORF 6	33.8	5.48	Putative nucleotide sugar epimerase (Q92VH2)	2E-32	30.0/297
ORF 7	27.6	5.91	Metallophosphoesterase (Q9HMV3)	5E-16	27.5/218
ORF 8	78.5	8.91	Putative acyltransferase (Q73SR3)	0.0	49.1/721
ORF 9	37.6	8.77	Putative glycosyltransferase Rv1518 (Q50590)	E-101	61.8/304
DrrC	28.5	11.69	Daunorubicin resistance protein C (Q9XCF9)	E-123	83.7/263

[a] Identity values were calculated by using BLASTX searches.

additional molecules of L-Rha and terminal amido-Hex. ORF 2 was assigned to methyltransferase and may be correlated with the synthesis of the *O*-methyl group at the C-2 position in the terminal amido-Hex. ORFs 4, 5, 7, and 8 were homologous to aminotransferase, carbamoyl phosphate synthase protein, metallophosphoesterase, and acyltransferase, respectively, and possibly relate to the biosynthesis of 2′-hydroxypropanoyl-amido in the terminal Hex. Taken together, this gene cluster may participate in the biosynthetic pathway of serotype 7 GPL, but further study will be required to define the function of each ORF that we have shown for the first time in this study.

GPL is one of the immunologically active molecules characteristic of MAC. Tassel et al. have reported that the core GPL seems to play a role in suppression of a mitogen-induced blastogenic response in spleen cells (35), and our previous study has shown that sera of patients with MAC disease contain immunoglobulin G (IgG), IgA, and IgM antibodies against the core of the GPL molecule (23). In addition, the immunomodulating activity of GPL on macrophage functions is serotype dependent (18, 34). The serotype 4 GPL promotes phagocytosis and inhibits phagosome-lysosome (P-L) fusion, whereas the GPLs of serotypes 9 and 16 exhibit no effect on phagocytosis and P-L fusion. The serotype 8 GPL shows concomitant stimulation of both phagocytosis and P-L fusion. The OSE of GPL may be involved in the mechanism of inhibition of P-L fusion, which is mediated through mannose receptors of macrophages (32). The serotype 4 GPL inhibited lymphoproliferative response to mitogens (18). Thus, host responses to GPLs vary with the MAC serotype.

The pathogenicity of GPL may comprise both a common peptide core and an OSE elongated from 6-d-Tal. GPL is a pleiotropic molecule and participates in the pathogenesis of MAC disease. Elucidation of the structure-activity relationship of GPL is required to better understand the pathogenesis.

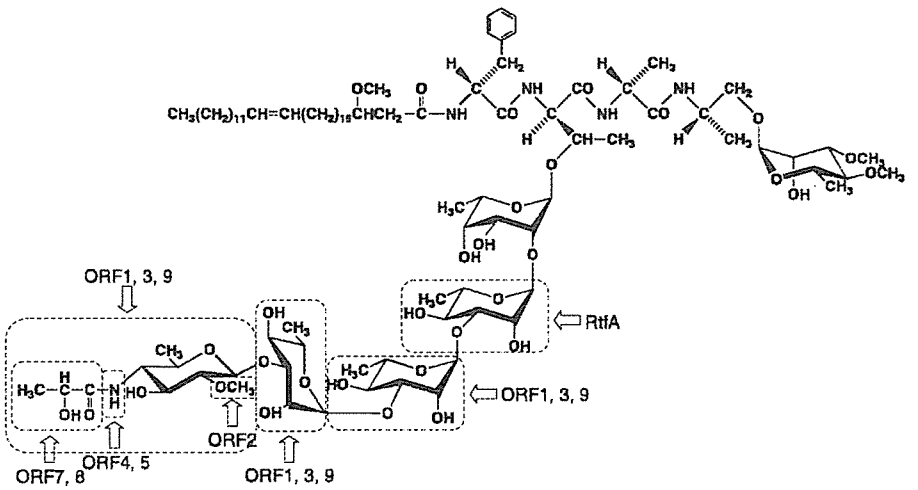

FIG. 8. Proposed structure of serotype 7 GPL and its predicted relationship to the genetic cluster.

ACKNOWLEDGMENTS

We thank Delphi Chatterjee, Michael McNeil, and Patrick J. Brennan (Department of Microbiology, Colorado State University, Fort Collins, CO) for helpful discussion on the structural analysis.

This work was supported by grants from the Ministry of Health, Labour and Welfare (Research on Emerging and Reemerging Infectious Diseases, Health Sciences Research Grants); the Ministry of Education, Culture, Sports, Science and Technology; the Osaka Tuberculosis Foundation; and The United States-Japan Cooperative Medical Science Program against Tuberculosis and Leprosy.

REFERENCES

1. **Aspinall, G. O., D. Chatterjee, and P. J. Brennan.** 1995. The variable surface glycolipids of mycobacteria: structures, synthesis of epitopes, and biological properties. Adv. Carbohydr. Chem. Biochem. **51**:169–242.
2. **Barrow, W. W., T. L. Davis, E. L. Wright, V. Labrousse, M. Bachelet, and N. Rastogi.** 1995. Immunomodulatory spectrum of lipids associated with *Mycobacterium avium* serovar 8. Infect. Immun. **63**:126–133.
3. **Belisle, J. T., L. Pascopella, J. M. Inamine, P. J. Brennan, and W. R. Jacobs, Jr.** 1991. Isolation and expression of a gene cluster responsible for biosynthesis of the glycopeptidolipid antigens of *Mycobacterium avium*. J. Bacteriol. **173**:6991–6997.
4. **Bozic, C. M., M. McNeil, D. Chatterjee, I. Jardine, and P. J. Brennan.** 1988. Further novel amido sugars within the glycopeptidolipid antigens of *Mycobacterium avium*. J. Biol. Chem. **263**:14984–14991.
5. **Brennan, P. J., and M. B. Goren.** 1979. Structural studies on the type-specific antigens and lipids of the *Mycobacterium avium·Mycobacterium intracellulare·Mycobacterium scrofulaceum* serocomplex. *Mycobacterium intracellulare* serotype 9. J. Biol. Chem. **254**:4205–4211.
6. **Brennan, P. J., and H. Nikaido.** 1995. The envelope of mycobacteria. Annu. Rev. Biochem. **64**:29–63.
7. **Camphausen, R. T., R. L. Jones, and P. J. Brennan.** 1986. Structure and relevance of the oligosaccharide hapten of *Mycobacterium avium* serotype 2. J. Bacteriol. **168**:660–667.
8. **Chatterjee, D., G. O. Aspinall, and P. J. Brennan.** 1987. The presence of novel glucuronic acid-containing, type-specific glycolipid antigens within *Mycobacterium* spp. Revision of earlier structures. J. Biol. Chem. **262**:3528–3533.
9. **Chatterjee, D., and K. H. Khoo.** 2001. The surface glycopeptidolipids of mycobacteria: structures and biological properties. Cell Mol. Life Sci. **58**: 2018–2042.
10. **Eckstein, T. M., J. T. Belisle, and J. M. Inamine.** 2003. Proposed pathway for the biosynthesis of serovar-specific glycopeptidolipids in *Mycobacterium avium* serovar 2. Microbiology **149**:2797–2807.
11. **Eckstein, T. M., F. S. Silbaq, D. Chatterjee, N. J. Kelly, P. J. Brennan, and J. T. Belisle.** 1998. Identification and recombinant expression of a *Mycobacterium avium* rhamnosyltransferase gene (*rtfA*) involved in glycopeptidolipid biosynthesis. J. Bacteriol. **180**:5567–5573.
12. **Enomoto, K., S. Oka, N. Fujiwara, T. Okamoto, Y. Okuda, R. Maekura, T. Kuroki, and I. Yano.** 1998. Rapid serodiagnosis of *Mycobacterium avium-intracellulare* complex infection by ELISA with cord factor (trehalose 6, 6′-dimycolate), and serotyping using the glycopeptidolipid antigen. Microbiol. Immunol. **42**:689–696.
13. **Falkinham, J. O., III.** 1996. Epidemiology of infection by nontuberculous mycobacteria. Clin. Microbiol. Rev. **9**:177–215.
14. **Fujita, Y., T. Doi, R. Maekura, M. Ito, and I. Yano.** 2006. Differences in serological responses to specific glycopeptidolipid-core and common lipid antigens in patients with pulmonary disease due to *Mycobacterium tuberculosis* and *Mycobacterium avium* complex. J. Med. Microbiol. **55**:189–199.
15. **Gerwig, G. J., J. P. Kamerling, and J. F. G. Vliegenthart.** 1978. Determination of the D and L configuration of neutral monosaccharides by high-resolution capillary G.L.C. Carbohydr. Res. **62**:349–357.
16. **Hakomori, S.** 1964. A rapid permethylation of glycolipid, and polysaccharide catalyzed by methylsulfinyl carbanion in dimethyl sulfoxide. J. Biochem. (Tokyo). **55**:205–208.
17. **Heidelberg, T., and O. R. Martin.** 2004. Synthesis of the glycopeptidolipid of *Mycobacterium avium* serovar 4: first example of a fully synthetic C-mycoside GPL. J. Org. Chem. **69**:2290–2301.
18. **Kano, H., T. Doi, Y. Fujita, H. Takimoto, I. Yano, and Y. Kumazawa.** 2005. Serotype-specific modulation of human monocyte functions by glycopeptidolipid (GPL) isolated from *Mycobacterium avium* complex. Biol. Pharm. Bull. **28**:335–339.
19. **Kaufmann, S. H.** 2001. How can immunology contribute to the control of tuberculosis? Nat. Rev. Immunol. **1**:20–30.
20. **Khoo, K. H., D. Chatterjee, A. Dell, H. R. Morris, P. J. Brennan, and P. Draper.** 1996. Novel *O*-methylated terminal glucuronic acid characterizes the polar glycopeptidolipids of *Mycobacterium habana* strain TMC 5135. J. Biol. Chem. **271**:12333–12342.
21. **Khoo, K. H., E. Jarboe, A. Barker, J. Torrelles, C. W. Kuo, and D. Chatterjee.** 1999. Altered expression profile of the surface glycopeptidolipids in drug-resistant clinical isolates of *Mycobacterium avium* complex. J. Biol. Chem. **274**:9778–9785.
22. **Kitada, S., R. Maekura, N. Toyoshima, N. Fujiwara, I. Yano, T. Ogura, M. Ito, and K. Kobayashi.** 2002. Serodiagnosis of pulmonary disease due to *Mycobacterium avium* complex with an enzyme immunoassay that uses a mixture of glycopeptidolipid antigens. Clin. Infect. Dis. **35**:1328–1335.
23. **Kitada, S., R. Maekura, N. Toyoshima, T. Naka, N. Fujiwara, M. Kobayashi, I. Yano, M. Ito, and K. Kobayashi.** 2005. Use of glycopeptidolipid core antigen for serodiagnosis of *Mycobacterium avium* complex pulmonary disease in immunocompetent patients. Clin. Diagn. Lab. Immunol. **12**:44–51.
24. **Krzywinska, E., and J. S. Schorey.** 2003. Characterization of genetic differences between *Mycobacterium avium* subsp. *avium* strains of diverse virulence with a focus on the glycopeptidolipid biosynthesis cluster. Vet. Microbiol. **91**:249–264.
25. **Maekura, R., Y. Okuda, A. Hirotani, S. Kitada, T. Hiraga, K. Yoshimura, I. Yano, K. Kobayashi, and M. Ito.** 2005. Clinical and prognostic importance of serotyping *Mycobacterium avium-Mycobacterium intracellulare* complex isolates in human immunodeficiency virus-negative patients. J. Clin. Microbiol. **43**:3150–3158.
26. **Maslow, J. N., V. R. Irani, S. H. Lee, T. M. Eckstein, J. M. Inamine, and J. T. Belisle.** 2003. Biosynthetic specificity of the rhamnosyltransferase gene of *Mycobacterium avium* serovar 2 as determined by allelic exchange mutagenesis. Microbiology **149**:3193–3202.
27. **McNeil, M., B. Gaylord, and P. J. Brennan.** 1988. *N*-Formylkansosaminyl-(1–3)-2-*O*-methyl-D-rhamnopyranose: the type-specific determinant of serovariant 14 of the *Mycobacterium avium* complex. Carbohydr. Res. **177**: 185–198.
28. **McNeil, M., A. Y. Tsang, and P. J. Brennan.** 1987. Structure and antigenicity of the specific oligosaccharide hapten from the glycopeptidolipid antigen of *Mycobacterium avium* serotype 4, the dominant *Mycobacterium* isolated from patients with acquired immune deficiency syndrome. J. Biol. Chem. **262**: 2630–2635.
29. **Miyamoto, Y., T. Mukai, N. Nakata, Y. Maeda, M. Kai, T. Naka, I. Yano, and M. Makino.** 2006. Identification and characterization of the genes involved in glycosylation pathways of mycobacterial glycopeptidolipid biosynthesis. J. Bacteriol. **188**:86–95.
30. **Patterson, J. H., M. J. McConville, R. E. Haites, R. L. Coppel, and B. Billman-Jacobe.** 2000. Identification of a methyltransferase from *Mycobacterium smegmatis* involved in glycopeptidolipid synthesis. J. Biol. Chem. **275**:24900–24906.
31. **Porcelli, S. A., and R. L. Modlin.** 1999. The CD1 system: antigen-presenting molecules for T cell recognition of lipids and glycolipids. Annu. Rev. Immunol. **17**:297–329.
32. **Shimada, K., H. Takimoto, I. Yano, and Y. Kumazawa.** 2006. Involvement of mannose receptor in glycopeptidolipid-mediated inhibition of phagosome-lysosome fusion. Microbiol. Immunol. **50**:243–251.
33. **Smith, I.** 2003. *Mycobacterium tuberculosis* pathogenesis and molecular determinants of virulence. Clin. Microbiol. Rev. **16**:463–496.
34. **Takegaki, Y.** 2000. Effect of serotype specific glycopeptidolipid (GPL) isolated from *Mycobacterium avium* complex (MAC) on phagocytosis and phagosome-lysosome fusion of human peripheral blood monocytes. Kekkaku **75**:9–18. [In Japanese.]
35. **Tassell, S. K., M. Pourshafie, E. L. Wright, M. G. Richmond, and W. W. Barrow.** 1992. Modified lymphocyte response to mitogens induced by the lipopeptide fragment derived from *Mycobacterium avium* serovar-specific glycopeptidolipids. Infect. Immun. **60**:706–711.

*rpoB*遺伝子と16S rRNA解析による抗酸菌同定の試み

鹿住 祐子　前田 伸司　菅原 勇

要旨：〔目的〕抗酸菌の同定に*rpoB*遺伝子シークエンスを利用できるか評価を行うために16S rRNAシークエンス（RIDOM）と比較し，さらにこの2つの方法を使い分けてDDH法にて菌種不明であった38臨床分離株を同定した。〔対象および方法〕ATCC標準菌株を中心とした抗酸菌（106株）と*Nocardia*属，*Rhodococcus*属，*Gordona*属合わせて計112株を用いて，*rpoB*遺伝子シークエンスと16S rRNAシークエンスを行った。そしてDDH法不明菌38臨床分離株のシークエンス結果を2つの方法のデータベースで相同性を調べ，菌種を決定した。〔結果・考察〕研究対象となった112株のうち16S rRNAシークエンス（RIDOM）では69.6%，*rpoB*遺伝子シークエンスでは89.3%が同定可能であった。16S rRNAシークエンス（RIDOM）では同定できない*M. kansasii*など11菌種を*rpoB*遺伝子データベースでは分けることが可能であったが，2つのシークエンスを用いても*M. tuberculosis*など12菌種を分けることができなかった。DDH法不明菌種の38株は*M. heckeshornense*，*M. branderi*など21菌種として同定され，両方の方法を組み合わせることによって97.4%が同定可能であった。

キーワーズ：抗酸菌の同定，16S rRNA，シークエンス，RIDOM，*rpoB*遺伝子，DDH法判定不能菌

はじめに

抗酸菌の同定は従来の生化学的・生物学的方法（以下，従来法）だけでは困難になってきている。近年，遺伝子を用いた方法が抗酸菌の研究に取り入れられるようになり[1][2]，抗酸菌は現在100種類以上同定でき，その威力を発揮している。同定方法として16S rRNAの塩基配列の相同性を調べる方法[3][4]，ミコール酸を分析する高速液体クロマトグラフィ（HPLC）[5]，PCR産物を制限酵素で切断して電気泳動する*hsp 65*（65-kDa heat shock protein）パターン解析[6]，日本の一般の病院検査室や検査センターなどでは16Sリボゾーム RNAの塩基配列の違いを利用したAccuProbe法[7]，基準株のDNAと被検株のDNAをハイブリダイゼーションし，相対類似度によって菌種を決定するDDHマイコバクテリア極東[8]（以下DDH法とする），目的とする菌種（例えば結核菌群）のDNAをPCR後に同定するアンプリコアマイコバクテリウム[9]，被検株のRNAを逆転写酵素でDNAにして同定する*Mycobacterium tuberculosis* Direct test（MTD）[10]などの遺伝子検査，培養菌が得られれば結核菌群であるかどうかの判定が15分でできる免疫クロマトグラフィ法のキャピリアTB[11]などが行われている。それぞれの方法には特徴があり，時間も従来法よりはるかに短縮されるようになった。しかしながら，抗酸菌にはこれらの方法を用いても同定できない菌種がなお多く存在する。今回われわれは一般的に広く使われている16S rRNAシークエンスのRIDOMデータベースによる解析とDNA依存性RNAポリメラーゼβサブユニットをコードしている*rpoB*遺伝子[12]~[14]のデータベースの利点を生かし，より精度の高い抗酸菌の同定を試みた。

材料と方法

使用菌株：American Type Culture Collection（ATCC）96菌種104株，Deutsche Sammlung von Mikroorganismen und Zellkulturen GmbH（DSMZ）2菌種4株，*Mycobacterium gordonae*グループ別臨床分離株3株，*M. leprae* 1株，計112株（標準菌株：Type strainは99株）を1%小川培地に発育させて研究材料とした。ただし，1%小川培地に発

結核予防会結核研究所抗酸菌レファレンスセンター

連絡先：鹿住祐子，結核予防会結核研究所抗酸菌レファレンスセンター病理検査科，〒204-8533 東京都清瀬市松山3-1-24
(E-mail: kazumi@jata.or.jp)
(Received 5 Apr. 2006/Accepted 8 Jun. 2006)

Table 1 Mycobacteria and other organisms used for the16S rRNA and *rpoB* sequence database in this study

	Species	Strain		Species	Strain
1.	*M. abscessus*	ATCC19977	57.	*M. komossense*	ATCC33013
2.	*M. acapulcensis*	ATCC14473	58.	*M. kubicae*	ATCC700732
3.	*M. africanum*	ATCC25420	59.	*M. lactis*	ATCC27356
4.	*M. agri*	ATCC27406	60.	*M. lentiflavum*	ATCC51985
5.	*M. aichiense*	ATCC27280	61.	*M. leprae*	Thai53*
6.	*M. alvei*	ATCC51304	62.	*M. madagascariense*	ATCC49865
7.	*M. asiaticum*	ATCC25276	63.	*M. mageritense*	ATCC700351
8.	*M. aurum*	ATCC23366	64.	*M. malmoense*	ATCC29571
9.	*M. austroafricanum*	ATCC33464	65.	*M. marinum*	ATCC927
10.	*M. avium* subsp. *avium*	ATCC25291	66.	*M. microti*	ATCC19422
11.	*M. avium* subsp. *paratuberculosis*	ATCC19698	67.	*M. montefiorense*	ATCCBAA-256
12.	*M. avium* subsp. *"suis"*	ATCC19978*	68.	*M. moriokaense*	ATCC43059
13.	*M. avium* subsp. *silvaticum*	ATCC49884	69.	*M. mucogenicum*	ATCC49650
14.	*M. botniense*	ATCC700701	70.	*M. neoaurum*	ATCC25795
15.	*M. bovis*	ATCC19210	71.	*M. nonchromogenicum*	ATCC19530
16.	*M. branderi*	ATCC51789	72.	*M. novium*	ATCC19619*
17.	*M. brumae*	ATCC51384	73.	*M. obuense*	ATCC27023
18.	*M. celatum*	ATCC51131	74.	*M. paraffinicum*	ATCC12670*
19.	*M. celatum* II	ATCC51130*	75.	*M. parafortuitum*	ATCC19686
20.	*M. chelonae* chemovar *niacinogenes*	ATCC35750*	76.	*M. peregrinum*	ATCC14467
21.	*M. chelonae* subsp. *chelonae*	ATCC35752	77.	*M. petroleophilum*	ATCC21497
22.	*M. chitae*	ATCC19627	78.	*M. phlei*	ATCC11758
23.	*M. chlorophenolicum*	ATCC49826	79.	*M. porcinum*	ATCC33776
24.	*M. chubuense*	ATCC27278	80.	*M. poriferae*	ATCC35087
25.	*M. confluentis*	ATCC49920	81.	*M. pulveris*	ATCC35154
26.	*M. conspicuum*	ATCC700090	82.	*M. rhodesiae*	ATCC27024
27.	*M. cookii*	ATCC49103	83.	*M. scrofulaceum*	ATCC19981
28.	*M. diernhoferi*	ATCC19340	84.	*M. senegalense*	ATCC35796
29.	*M. duvalii*	ATCC43910	85.	*M. septicum*	ATCC700731
30.	*M. engbaekii*	ATCC27353	86.	*M. shimoidei*	ATCC27962
31.	*M. fallax*	ATCC35219	87.	*M. shinshuense*	ATCC33728
32.	*M. farcinogenes*	ATCC35753	88.	*M. simiae*	ATCC25275
33.	*M. flavescens*	ATCC14474	89.	*M. smegmatis*	ATCC19420
34.	*M. fortuitum* subsp. *acetamidolyticum*	ATCC35931	90.	*M. smegmatis*	ATCC700084*
35.	*M. fortuitum* subsp. *fortuitum*	ATCC6841	91.	*M. sphagni*	ATCC33027
36.	*M. fortuitum* subsp. *fortuitum*	ATCC49403	92.	*M. szulgai*	ATCC35799
37.	*M. fortuitum* subsp. *fortuitum*	ATCC49404	93.	*M. terrae*	ATCC15755
38.	*M. gadium*	ATCC27726	94.	*M. terrae*	DSM43540*
39.	*M. gallinarum*	ATCC19710*	95.	*M. terrae*	DSM43541*
40.	*M. gastri*	ATCC15754	96.	*M. terrae*	DSM43542*
41.	*M. genavense*	ATCC51233	97.	*M. thermoresistibile*	ATCC19527
42.	*M. gilvum*	ATCC43909	98.	*M. tokaiense*	ATCC27282
43.	*M. goodii*	ATCC700504	99.	*M. triplex*	ATCC700071
44.	*M. gordonae*	ATCC14470	100.	*M. triviale*	ATCC23292
45.	*M. gordonae* group B**	KK33-08*	101.	*M. tuberculosis* H37Rv	ATCC27294
46.	*M. gordonae* group C**	KK33-53*	102.	*M. ulcerans*	ATCC19423
47.	*M. gordonae* group D**	KK33-46*	103.	*M. vaccae*	ATCC15483
48.	*M. haemophilum*	ATCC29548	104.	*M. valentiae*	ATCC29356
49.	*M. hassiacum*	ATCC700660	105.	*M. wolinskyi*	ATCC700010
50.	*M. heckeshornense*	DSM44428	106.	*M. xenopi*	ATCC19250
51.	*M. heidelbergense*	ATCC51253	107.	*Nocardia asteroides*	ATCC19247
52.	*M. hiberniae*	ATCC49874	108.	*Rhodococcus equi*	ATCC6939
53.	*M. interjectum*	ATCC51457	109.	*Gordona aichiensis*	ATCC33611
54.	*M. intermedium*	ATCC51848	110.	*Gordona aurantiaca*	ATCC25938
55.	*M. intracellulare*	ATCC13950	111.	*Gordona bronchialis*	ATCC25592
56.	*M. kansasii*	ATCC12478	112.	*Gordona terrae*	ATCC25594

*These are not type strains.
**Refer to ref.16).

育困難な菌株はMiddlebrook 7H9液体培地にて培養し，*M. leprae*はDNA抽出液を供与されたためこれを用いた。Table 1に用いた菌種の内訳を示した。

（1）DNAの抽出

1.5 ml用のビーズ入りプラスチックチューブに，10% Sodium dodecyl sulfate（SDS）600 μlを入れ，小川培地発育菌の1白金耳を加え，液体培地発育菌は遠心沈殿した後の沈渣を加え，95℃，10分間加温した。これに600 μlのフェノール・クロロホルム等量混合液を加え，80秒間撹拌した。さらに4,200 rpm 5分間遠心沈殿。上清500 μlをとって別の容器に移し，クロロホルム500 μl加えて混和，3,000 rpm 5分間遠心沈殿。上清を360 μl別の容器に移し，クロロホルム360 μl加え，10,000 rpm 10分間遠心沈殿。上清250 μlにエタノール500 μl加え，－80℃にて20分間静置。10,000 rpm 10分間遠心沈殿。エタノールを捨て，風乾し，TE 100 μlに浮遊させてDNA抽出液として使用した。

（2）16S rRNAシークエンス・RIDOMデータベース解析[15]

16S rRNA遺伝子は染色体DNAの1/1,000程度で，全長が約1,500 bpほどあり，今回シークエンスを調査したのはこのうちの446 bpである。

DNA抽出液のゲノムDNA2.5 μlを用いてPCRの反応を行った。PCR反応には10倍 Buffer 5 μl, 10 mM dNTP 2 μl, 滅菌蒸留水38 μl, Ampli *Taq* Gold（Roche Diagnostics, 東京）0.5 μl（2.5 units），プライマー2 μlを混和して反応溶液とした。増幅にはプライマー264（5'-TGC ACA CAG GCC ACA AGG GA-3'）およびプライマー285（5'-GAG AGT TTG ATC CTG GCT CAG-3'）を各々0.1 nmol使用した[9]。PCR反応条件は，94℃ 30秒間，60℃ 30秒間，72℃ 1分30秒間を40サイクル行った。PCR産物をアガロースゲル電気泳動にて確認後，精製はスピンカラム（SUPREC TM-02, TAKARA, TAKARA SHUZO Co., LTD）を用いた。ダイレクトシークエンスはBig Dye terminator（ABI 4303153 Big Dye Terminator cycle Fs Ready Reaction Kit 1,000）4 μl, 3.2 pmol プライマー285を2 μl, 5×Buffer 2 μl, 滅菌蒸留水11 μl, 精製されたPCR産物1 μlを混和し，添付のプロトコールどおりに行い，ABI 310にて実施し，得られた塩基配列データはRibosomal Differentiation of Microorganisms（RIDOM）(http://www.ridom-rdna.de/)にて相同性を調べ，98%以上の一致をもって，その菌種として同定した。

（3）*rpoB*遺伝子シークエンス・*rpoB*遺伝子データベース解析

*M. tuberculosis*の*rpoB*遺伝子は全長が3,519 bpあり，RNAポリメラーゼのβサブユニットをコードしている。この多型性を抗酸菌の同定に利用した。Kimらの報告[13][14]による*rpoB*遺伝子上のアミノ酸で444から454番目（大腸菌での番号）のHighly conserved regions（HCR）5領域内にプライマーP1，547から577番目のHCR 6領域内にプライマーP2を設計し，306 bpのシークエンスの決定を行った。

PCR反応溶液は16S rRNAシークエンスの方法に準じた。*rpoB*の増幅[13]にはプライマーP1（5'-CGA CCA CTT CGG CAA CCG-3'）およびプライマーP2（5'-TCG ATC GGG CAC ATC CGG-3'）を各々3.2 pmol使用した。PCR反応条件は，94℃ 1分間，66℃ 1分間，72℃ 1分間を40サイクル行った。PCR産物を確認後，精製はスピンカラムを用い，ダイレクトシークエンスはプライマーP1とP2それぞれをBig Dye terminatorを用いてABI 310にて実施した。*rpoB*遺伝子シークエンスについてはGENETYX-WIN Ver.5.2（Software Development社）にて当研究所にて作成した*rpoB*遺伝子データベースを使用し，GENETYX-PDB Ver.4.1（Software Development社）で相同性を調べ，99%以上の塩基配列の一致をもって菌種を同定した。

（4）DDH法[8]

市販キットの使用説明書（DDHマイコバクテリア'極東'：極東製薬）に従って行った。フェノール・クロロホルム試薬キットによってDNAを抽出し，ビオチンで標識，1本鎖にした後，これを予めマイクロプレートに固定されている以下の18菌種の基準株と2時間ハイブリダイゼーションを行った。固定されている菌種は，*M. tuberculosis* complex（結核菌群：BCG），*M. kansasii*, *M. marinum*, *M. simiae*, *M. scrofulaceum*, *M. gordonae*, *M. szulgai*, *M. avium*, *M. intracellulare*, *M. gastri*, *M. xenopi*, *M. nonchromogenicum*, *M. terrae*, *M. triviale*, *M. fortuitum*, *M. chelonae*, *M. abscessus*, *M. peregrinum*である。洗浄を繰り返し，発色試薬を加え，630 nmで吸光度を測定した。1番強く発色したウエルと2番目に強く発色したウエルの吸光度の相対類似度が70%以下であるとき，1番強く発色したウエルの基準株と被検株が同じ菌種であると判定し，18菌種のうちの1つの菌名に決定した。なお，このとき，1番強く発色したウエルの吸光度と対照ウエル（大腸菌のDNA）の吸光度の差が1.9倍なければならない。技術的誤りがなく，以上2つの条件を満たさない場合，DDH法判定不能菌と判定した。

結　果

（1）16S rRNAシークエンス・RIDOMデータベース解析の結果

Table 1の112株のうちRIDOMデータベースでは*M. kansasii*と*M. gastri*のように100%一致するため分けることができなかった株をTable 2とTable 3に示した。

Table 2 Comparison of homology by 16S rRNA and *rpoB* sequencing

16S rRNA sequencing (RIDOM)		*rpoB* sequencing
Homology		Homology
100% *M. kansasii* and *M. gastri*	→	100% *M. kansasii* vs 93.8% *M. gastri*
100% *M. abscessus* and *M. chelonae*	→	100% *M. abscessus* vs 97.1% *M. chelonae*
100% *M. fortuitum* ATCC49404 and *M. porcinum*	→	100% *M. fortuitum* ATCC49404 vs 96% > *M. porcinum*
100% *M. peregrinum* and *M. septicum*	→	100% *M. peregrinum* vs 97.4% *M. septicum*
100% *M. farcinogenes*, *M. senegalense* and *M. fortuitum* ATCC49403	→	100% *M. farcinogenes* vs 94% > *M. senegalense*/98% *M. fortuitum* ATCC49403

Table 3 List of unidentified strains by 16S rRNA and *rpoB* sequencing

100% same Homology
1. *M. tuberculosis*, *M. bovis*, *M. africanum* and *M. microti*
2. *M. avium* subsp. *avium*, *M. avium* subsp. *silvaticum*, *M. avium* subsp. "*suis*" and *M. avium* subsp. *paratuberculosis*
3. *M. marinum* and *M. ulcerans*
4. *M. fortuitum* (ATCC6841) and *M. fortuitum* subsp. *acetamidolyticum*

Table 2はRIDOMデータベースによって解析できなかったが*rpoB*遺伝子データベースにおいて菌種決定可能であった株で，Table 3はRIDOMデータベースと*rpoB*遺伝子データベースの両方を用いても分けることのできない4つのグループである。Table 2と3のRIDOMの結果はTurenneら[3]と同じであった。さらに*M. celatum* II (ATCC51130)，*M. chelonae* chemovar *niacinogenes*，*M. montefiorense*，*M. lactis*，*M. novium*はRIDOMデータベースに登録されていないためこれらを同定することはできなかった。*N. asteroides*，*R. equi*，*G. aichiensis*，*G. aurantiaca*，*G. bronchialis*，*G. terrae*は抗酸菌ではないためPCRでDNA産物が生成されなかった。

従ってTable 1の112株のうち，相同性が100%一致しているため分けられない23株 (Table 2と3) とRIDOMに登録されていない5株，そして抗酸菌ではない6株計34株が同定できなかったため，同定可能な株はTable 1に記載されている菌株の69.6%であった。

(2) *rpoB*遺伝子シークエンス・*rpoB*遺伝子データベース解析の結果

RIDOMデータベースでは同定できないTable 2の11株と抗酸菌ではない6株を*rpoB*遺伝子データベースで分けることができた。しかしながら，Table 3の12株については分けることはできなかったため，Table 1の112株のうち*rpoB*遺伝子データベースで分けることが可能であったのは89.3%であった。

(3) DDH法により判定不能であった臨床分離株の同定

これら2つのシークエンスを決定する方法を用いたDDH法判定不能の38臨床分離株の同定結果をTable 4に示した。Teble 4のRIDOMデータベースの結果は相同性が98%以上，*rpoB*遺伝子データベースにおいては99%以上の菌種を示した。

以前，われわれは*rpoB*遺伝子シークエンスを用いて*M. gordonae*を4つのグループに分けた[10]。今回の*M. gordonae* 5株 (No. 60, 330, 353, 469, 528) はRIDOMデータベースで*M. gordonae*と同定したが，*rpoB*遺伝子シークエンスを用いた方法ではATCC14470 (ATCC Type Strain) と一致せず，Bグループ1株，Cグループ2株，Dグループ2株であった。

No.728はRIDOMデータベースによって*M. malmoense*と*M. szulgai*が候補となったが，*rpoB*遺伝子データベースでは99.7% *M. malmoense*で*M. szulgai*との相同性は90.5%となり*M. szulgai*は除外された。No. 600はRIDOMデータベースでは*M. porcinum* (ATCC33776) と*M. fortuitum* (ATCC49404) の両方と99.76%の塩基配列が一致し，相同性が100%であったため決定できなかった。しかし，*rpoB*遺伝子データベースにおいて*M. fortuitum* (ATCC 49404) との一致率は94.12%と低く，*M. fortuitum*は除かれた。

しかし，RIDOMデータベースによって同定可能であったが，*rpoB*遺伝子データベースにおいて不明となった例があった。No. 660はRIDOMデータベースによって99.7% *M. terrae*と同定されたが，*rpoB*遺伝子データベースではATCC15755 (ATCC Type Strain: *M. terrae*) とは96.1%であった。Table 5にNo. 660とATCC15755の塩基配列の比較を示した。No. 660 (上段) とATCC15755 (下段) には12カ所の塩基配列に違いがあり，306塩基のうち一致した数が294塩基 (96.1%) であったため不一致と判断した。そして他にもこの株と99%以上一致した菌種がなく，菌種不明となった。

RIDOMデータベースにおいて該当なしとなった1株 (No. 481)，抗酸菌ではなかったためPCRできなかった

Table 4 Candidate mycobacteria determined by DNA sequencing analyses of the 16S rRNA gene and *rpoB* in unidentified ones with DDH method.

Strains	16S rRNA (more than 98%)	*rpoB* (more than 99%)
808	*M. branderi* (99.53)	*M. branderi* (100)
481	None	*M. celatum* II (99.7)
374	*M. chelonae* and *M. abscessus* (100)	*M. chelonae* chemovar *niacinogenes* (100)
405	*M. chelonae* and *M. abscessus* (100)	*M. chelonae* chemovar *niacinogenes* (100)
211	*M. conspicuum* (100)/*M. szulgai* (98.1)	*M. conspicuum* (100)
661	*M. conspicuum* (100)	*M. conspicuum* (100)
521	*M. engbaekii, M. hiberniae* and *M. lactis* (99.73)/*M. terrae* (98.55)	*M. hiberniae* and *M. lactis* (99.3)/*M. engbaekii* (99.0)
353	*M. gordonae* (99.77)	*M. gordonae* B-group (99.7)
469	*M. gordonae* (100)	*M. gordonae* C-group (99.7)
528	*M. gordonae* (100)	*M. gordonae* C-group (99.7)
60	*M. gordonae* (99.32)	*M. gordonae* D-group (99.7)
330	*M. gordonae* (100)	*M. gordonae* D-group (99.7)
50	*M. heckeshornense* (100)	*M. heckeshornense* (99.7)
759	*M. heckeshornense* (100)	*M. heckeshornense* (100)
727	*M. intermedium* (99.77)	*M. intermedium* (99.7)
718	*M. lentiflavum* (100)/*M. simiae* (98.79)	*M. lentiflavum* (100)
739	*M. lentiflavum* (99.76)/*M. simiae* (98.56)	*M. lentiflavum* (99.4)
902	*M. lentiflavum* (100)/*M. simiae* (98.77)	*M. lentiflavum* (100)
667	*M. mageritense* (99.08)	*M. mageritense* (99.7)
686	*M. mageritense* (99.52)/*M. wolinskyi* (98.07)	*M. mageritense* (100)
396	*M. malmoense* (98.64)	*M. malmoense* (100)
728	*M. malmoense* (99.47)/*M. szulgai* (99.21)	*M. malmoense* (99.7)
242	*M. mucogenicum* (100)/*M. farcinogenes* (99.52)	*M. mucogenicum* (99.3)
277	*M. mucogenicum* (99.03)/*M. farcinogenes* (98.54)	*M. mucogenicum* (99.7)
298	*M. mucogenicum* (98.83)/*M. farcinogenes* (98.36)	*M. mucogenicum* (99.0)
692	*M. mucogenicum* (99.73)/*M. farcinogenes* (98.32)	*M. mucogenicum* (99.0)
221	*M. neoaurum* (100)/*M. lacticola* (99.79)	*M. neoaurum* (99.3)
229	*M. neoaurum* (100)/*M. lacticola* (99.79)	*M. neoaurum* (99.3)
55	*M. paraffinicum* (99.77)/*M. scrofulaceum* (99.40)	*M. paraffinicum* (99.7)
600	*M. porcinum* and *M. fortuitum* (99.76)	*M. porcinum* (99.7)
85	None	*Gordona aichiensis* (99.7)
538	*M. shimoidei* (100)	*M. shimoidei* (100)
312	*M. szulgai* (98.90)	*M. szulgai* (99.7)
660	*M. terrae* (99.70)	None*
394	*M. triplex* (100)/*M. genavense* (99.01)	*M. triplex* (99.7)
431	*M. triplex* (100)/*M. genavense* (98.77)	*M. triplex* (99.7)
482	*M. triplex* (99.3)/*M. genavense* (98.37)	*M. triplex* (99.3)
520	*M. wolinskyi* (100)	*M. wolinskyi* (99.3)

(%) Similarity
*See to Table 5

Table 5 Comparison of *rpoB* gene sequences between a clinical isolate and *M. terrae* type strain

```
Query:   1  TGCGCACCGTGGGCGAGCTGATCCAGAACCAGATCCGGGTCGGGCTGTCCCGGATGGAGC  60
Sbjct:   1  TGCGCACGGTGGGTGAGCTGATCCAGAACCAGATCCGGGTCGGGTTGTCCCGGATGGAGC  60
Query:  61  GCGTGGTCCGCGAGCGGATGACCACCCAGGACGTCGAGGCCATCACGCCGCAGACCCTGA 120
Sbjct:  61  GTGTGGTCCGCGAGCGGATGACCACCCAGGACGTCGAGGCCATCACGCCGCAGACCCTGA 120
Query: 121  TCAACATCCGCCCGGTGGTCGCCGCGATCAAGGAGTTCTTCGGCACCAGCCAGCTCTCCC 180
Sbjct: 121  TCAACATCCGCCCGGTGGTCGCCGCGATCAAGGAGTTCTTCGGCACCAGCCAGCTCTCGC 180
Query: 181  AGTTCATGGACCAGAACAACCCGCTGTCGGGTCTGACCCACAAGCGCCGCCTGTCGGCGC 240
Sbjct: 181  AGTTCATGGACCAGAACAACCCGCTGTCGGGTCTGACCCACAAGCGCCGGCTGTCGGCGC 240
Query: 241  TGGGGCCGGGCGGTCTGTCGCGTGAGCGGGCCGGGCTGGAAGTTCGTGACGTGCACCCGT 300
Sbjct: 241  TGGGCCCGGGTGGTCTGTCCCGTGAGCGGGCCGGGCTTGAGGTCCGTGACGTGCACCCGT 300
Query: 301  CCCACT 306
Sbjct: 301  CCCACT 306
```

Query: Clinical isolate: No.660
Sbjct: *M. terrae* ATCC15755

1株（No.85），そして相同性が同じ候補が複数あった4株（No.374, 405, 521, 600）を除き，今回のDDH不明菌の38株中32株（84.2%）が同定可能であった。また*rpoB*遺伝子データベースでは38株から該当なしとなった1株（No.660）と相同性が同じ候補が複数あったNo.521を除いた36株（94.7%）が同定可能であった。そしてRIDOMデータベースと*rpoB*遺伝子データベースの両方，またはいずれかで同定できたのは97.4%であった。

考　察

RIDOMデータベースで検索できる抗酸菌は154株（109種類）と抗酸菌の多くを同定することができ，インターネットで誰でもアクセスできるため世界に広がっている。遺伝子検査の利点として，①従来法による同定試験では数カ月を要した。しかし，シークエンスを決定することによって1日～2日で検査結果を得ることができる。②従来法には大量の菌量を必要とするが*M. malmoense*のように卵培地における発育の悪い株もあり，必要な菌量が得られないことがある。遺伝子検査の中でも特にPCRなどを利用する場合，微量で検査が可能である。③従来法は鑑別培地への接種する菌量・判定が難しいという欠点をもつが，遺伝子検査法は手技がマニュアル化されている。などがあげられる。

しかしながら，従来法[17)~19)]を否定することはできない。RIDOMデータベースと*rpoB*遺伝子データベースで同定できない菌が従来法で同定可能な場合がある。例えば，*M. shinshuense*は*M. marinum*・*M. ulcerans*とは1塩基違いで非常に近く，RIDOMデータベースと*rpoB*遺伝子データベースを用いてもこれらから明確に分けることができないが，光発色試験・発育速度・アリルスルファターゼ試験・薬剤に対する感受性パターンなどが大切な鍵となる[20)]。また，16S rRNAシークエンスで分けることのできない*M. kansasii*と*M. gastri*も光発色試験と硝酸還元試験が大変参考となる。しかし，遺伝子検査と従来法の結果が一致するとは限らず〔*M. cheronae* chemovar *niacinogenes*（ATCC35750）はナイアシンテスト陽性であったが，Table 4の*M. cheronae* chemovar *niacinogenes*と同定されたNo.374と405は陰性であった〕，特に検出稀な菌種が得られたときはコロニー形態・生物学的性状・生化学的性状・薬剤感受性試験のパターンなどを標準菌株と比較しながら確認する必要がある。

*rpoB*遺伝子データベースは，①RIDOMデータベースでは分けることのできないTable 2の菌種を同定できる。②RIDOMデータベースで複数の候補があげられた*M. lentiflavum*などを1菌種にしぼることが可能である。③*M. celatum* Ⅱ（No.481）と*M. chelonae* chemovar *niacinogenes*（No.374，405）と抗酸菌ではない*G. aichiensis*（No. 85）のようにRIDOMデータベースに登録されていない菌種の同定に役立つ。④以前，われわれは*M. gordonae*を*rpoB*遺伝子シークエンスによって4つのグループに分け*M. gordonae*には遺伝学的多型性があると考えた。そして*M. terrae*にも*M. gordonae*のような多型性の可能性があると考えられ，*M. terrae*のDSM43540，DSM43541とDSM43542はRIDOMデータベースによってATCC15755と分けることができなかったが，*rpoB*遺伝子シークエンスではこの4株を分けることができた。*rpoB*遺伝子シークエンスはこのような多型性の分類に役立つと思われる。

しかし，*rpoB*遺伝子シークエンスデータベースはNo. 221，229の候補となった*M. lacticola*のようにRIDOMデータベースに登録されていて，当研究所の*rpoB*遺伝子データベースにデータのない菌種はこれによって同定することができない。今後，さらなるデータ蓄積が望まれる。

非結核性抗酸菌の病原性については不明なものも多いが，今回の研究で菌種の判明したTable 4の菌種については，文献[2)21)]によると*M. celatum*の初めての分離は2名のHIV患者からであったが，日和見的に病原性があると言われる。*M. conspicuum*も免疫不全者から分離され，*M. porcinum*という菌は1983年に束村によってブタに結核のようなリンパ節炎を起こしたとして発表された。発育の速い*M. wolinskyi*は骨折後の骨髄炎に関係し，*M. szulgai*は稀にヒトに肺結核類似症を引き起こす。そして肺疾患患者から分離された*M. shimoidei*もヒトに対して病原性があると考えられている。コロニーが黄色く色のつく*M. lentiflavum*は1996年に脊椎椎間板炎病巣から検出され，さらに汚染された気管支鏡の使用が原因と考えられた臨床材料からも分離され，胃液・喀痰・尿からも得られている。*M. triplex*は肝臓移植を受けた若い女性の心嚢液と腹水から検出され，そして免疫機能正常な肺疾患患者からも分離されたことがある。さらに肺感染症の原因と考えられた*M. malmoense*[22)]と*M. intermedium*[23)]，右肺の空洞病変のある患者から分離されことがある*M. branderi*[24)]，1993年にヨーロッパで右上肺葉に空洞のある30歳の女性の喀痰から検出された*M. xenopi*-likeは2000年に*M. heckeshornense*[25)]として発表され，この時，病原性があったと考えられた[26)]。*M. mucogenicum*については検査室内汚染[21)]とも言われるが，免疫機能に異常のない82歳と23歳の男性の髄液から検出され，2症例とも入院後短期間で死亡したと報告された[27)]。このように稀な非結核性抗酸菌の中にも病原性をもつものが少なくなく，特に患者側の免疫機能低下によって原因菌ともなりうる。このようなことから非結核性抗酸菌の同定は重要性を増すものと考えられる。

ま と め

結核蔓延時代には結核菌と他の抗酸菌という分け方であったが，近年は枠を超えて結核菌だけでなく非結核性抗酸菌の同定も重要性を増してきている。現在までにわれわれの研究所で所有している *rpoB* 遺伝子データベースはATCC・DSMのType strain (Table 1) が主であるが，今後の課題として検出の稀な菌種とこれらの方法によってもまだ菌種不明とされた株のデータの蓄積を行い，不明菌の解析に努めたい。

医療機関の実験室・検査室でこれらの方法を用いて同定を行うとき，16S rRNA・*rpoB* 遺伝子のシークエンスの決定は微量のDNAから同定することができるため非常に有用であるが，PCRを使うため，実験室内汚染 (Cross contamination) を常に考慮しなければならない。さらに1本の培地上に抗酸菌が複数種類混在する可能性もあり，このため検体の種類と検出回数・コロニーの形態学的特徴・分離培養時の状況も重要な情報となる。

最後にRIDOMデータベースに登録されている154株とわれわれの *rpoB* 遺伝子データベースに登録されている112株の菌の種類に違いがあり，この2つの方法の特徴を理解したうえで利点を使い分け，従来法にて確認することで分析能力を増すことができると考えられる。

謝　辞

この研究にあたって元国立療養所中部病院 東村道男先生に23株，元BCG研究所 故工藤祐是先生にH37Rv，国立感染症研究所ハンセン病研究センター 松岡正典先生に *M. leprae* を分与して頂き深謝致します。そしてこの論文を作成するにあたりご高閲頂いた前結核予防会結核研究所基礎研究部長 阿部千代治先生に深謝致します。

文　献

1) Tortoli E, Bartoloni A, Bottger EC, et al.: Burden of unidentifiable mycobacteria in a reference laboratory. J Clin Microbiol. 2001 ; 39 : 4058–4065.
2) Tortoli E: Impact of genotypic studies on mycobacterial taxonomy : the new mycobacteria of the 1990s. Clin Microbiol Rev. 2003 ; 16 : 319–354.
3) Turenne CY, Tschetter L, Wolfe J, et al.: Necessity of quality-controlled 16S rRNA gene sequence databases: identifying nontuberculous *Mycobacterium* species. J Clin Microbiol. 2001 ; 39 : 3637–3648.
4) Springer B, Stockman L, Teschner K, et al.: Two-laboratory collaborative study on identification of mycobacteria: molecular versus phenotypic methods. J Clin Microbiol. 1996 ; 34 : 296–303.
5) Butler WR, Guthertz LS: Mycolic acid analysis by high-performance liquid chromatography for identification of *Mycobacterium* species. Clin Microbiol Rev. 2001 ; 14 : 704–726.
6) Brunello F, Ligozzi M, Cristelli E: Identification of 54 Mycobacterium species by PCR-restriction fragment length polymorphism analysis of the hsp65 gene. J Clin Microbiol. 2001 ; 39 : 2799–2806.
7) Tomioka H, Saito H, Sato K: Identification of *Mycobacterium avium* complex strains belonging to serovars 21–28 by three commercial DNA probe tests. Tuber Lung Dis. 1993 ; 74 : 91–95.
8) 江崎孝行：DNAを使った抗酸菌の迅速同定．結核．1992 ; 67 : 803–806.
9) 阿部千代治，齋藤由美子，本山禎二，他：アンプリコアマイコバクテリウムキットの評価に関する共同研究．結核．1997 ; 72 : 181–186.
10) 大角光彦，豊田丈夫，川城丈夫，他：核酸 (ribosomal RNA) 増幅を利用した結核菌検出の臨床的有用性に関する検討．結核．1996 ; 71 : 700–702.
11) Hasegawa N, Miura T, Ishii K, et al.: New simple and rapid test for culture confirmation of *Mycobacterium tuberculosis* complex: a multicenter study. J Clin Microbiol. 2002 ; 40 : 908–912.
12) Boor KJ, Duncan ML, Price CW: Genetic and transcriptional organization of the region encoding the beta subunit of Bacillus subtilis RNA polymerase. J Biol Chem. 1995 ; 270 : 20329–20336.
13) Kim BJ, Lee SH, Lyu MA, et al.: Identification of mycobacterial species by comparative sequence analysis of the RNA polymerase gene (*rpoB*). J Clin Microbiol. 1999 ; 37 : 1714–1720.
14) Kim BJ, Lee KH, Park BN, et al.: Differentiation of mycobacterial species by PCR-restriction analysis of DNA (342 base pairs) of the RNA polymerase gene (*rpoB*). J Clin Microbiol. 2001 ; 39 : 2102–2109.
15) Harmsen D: RIDOM: Ribosomal Differentiation of Medical Micro-organisms Database. Nucleic Acids Res. 2002 ; 30 : 416–417.
16) Itoh S, Kazumi Y, Takahashi M: Heterogeneity of RNA polymerase gene (*rpoB*) sequences of *Mycobacterium gordonae* clinical isolates identified with a DNA probe kit and by conventional methods. J Clin Microbiol. 2003 ; 41 : 1656–1663.
17) Tsukamura M: A review of the methods of identification and differentiation of mycobacteria. Rev Infect Dis. 1981 ; 3 : 841–861. Review.
18) Public health mycobacteriology: A Guide for the Level Ⅲ Laboratory. Department of Health and Human services. Center for Disease Control, Atlanta GA 30333.
19) Wayne LG, Good RC, Bottger EC : Semantide-and chemotaxonomy-based analyses of some problematic phenotypic clusters of slowly growing mycobacteria, a cooperative study of the International Working Group on Mycobacterial Taxonomy. Int J Syst Bacteriol. 1996 ; 46 : 280–297.

20) 鹿住祐子, 大友幸二, 高橋光良, 他：皮膚から分離された*Mycobacterium shinshuense*の細菌学的解析. 結核. 2004；79：437-441.
21) Barbara A, Brown-Elliott, Richard J, et al.: Clinical and taxonomic status of pathogenic nonpigmented or late-pigmenting rapidly growing mycobacteria. Clin Microbiol Rev. 2002；15：716-746.
22) 熊本光孝, 西山秀樹, 鹿住祐子, 他：*Mycobacterium malmoense*による肺感染症の1例. 日本呼吸器学会雑誌. 2005；43：454-458.
23) Ito A, Kishi F, Saito N, et al.: Pulmonary *Mycobacterium intermedium* disease in an elderly man with healed pulmonary tuberculosis. J Clin Microbiol. 2005；43：1473-1474.
24) Sugawara I, Kazumi Y, Otomo K, et al.: *Mycobacterium branderi* Isolated from Pus of a Right Pulmonary Cavitary lesion. Japanese Journal of Infectious Diseases. 2005；58：187-188.
25) Roth A, Reischl U, Schonfeld N, et al.: *Mycobacterium heckeshornense* sp. nov., A new pathogenic slowly growing *Mycobacterium* sp. Causing cavitary lung disease in an immunocompetent patient：J Clin Microbiol. 2000；38：4102-4107.
26) 鹿住祐子, 和田雅子, 菅原 勇, 他：2症例から細菌学的に同定された*Mycobacterium heckeshornense*について. 結核. 2006；81：ページ未定.
27) Adekambi T, Foucault C, La Scola B, et al.: Report of two fatal cases of *Mycobacterium mucogenicum* central nervous system infection in immunocompetent patients. J Clin Microbiol. 2006；44：837-840.

Original Article

IDENTIFICATION OF MYCOBACTERIA BY SEQUENCING OF *rpoB* GENE AND 16S rRNA

Yuko KAZUMI, Shinji MAEDA, and Isamu SUGAWARA

Abstract [Purpose] To classify a specific *Mycobacterium* among various mycobacteria utilizing sequencing of *rpoB* gene. To classify mycobacteria not identified by DNA-DNA hybridization (DDH) using sequencing of *rpoB* and 16S rRNA gene.

[Objects and methods] Classification of 106 Mycobacteria strains, one *Nocardia* strain, one *Rhodococcus* strain, four *Gordona* strains was made by using partial sequencing of *rpoB* and 16S rRNA (RIDOM). Thereafter, 38 mycobacteria clinical strains not identified by DDH were classified utilizing the DNA sequencing data.

[Results] Pairs of *M. kansasii* and *M. gastri*, *M. abscessus* and *M. chelonae*, *M. fortuitum* (ATCC49404) and *M. polcinum*, *M. peregrinum* and *M. septicum*, *M. farucinogense* and *M. senegalense* and *M. fortuitum* (ATCC49403), *Rhodococcus*, *Nocardia* and *Gordona* strains were classified using sequencing of *rpoB* gene. Even though sequencing of *rpoB* and 16S rRNA gene was utilized, it was impossible to classify *M. tuberculosis* complex, *M. avium* family, *M. marinum* and *M. ulcerans*, and *M. fortitum* subsp. *fortuitum* and *M. fortuitum* subsp. *acetamidolyticus*.

The 38 mycobacteria clinical strains not identified by DDH were successfully classified using sequencing of both *rpoB* and 16S rRNA. These sequencing analyses showed that *M. heckeshornense*, *M. branderi*, *M. intermedium*, *M. shimoidei*, *M. wolinskyi*, *M. malmoense* and *M. lentiflavum* could be identified. Thirty six clinical isolates (94.7%) and 32 clinical isolates (84.2%) were identified by *rpoB* sequencing and 16S rRNA sequencing (RIDOM), respectively.

[Conclusion] The classification ratio of mycobacteria including *Nocardia*, *Rhodococcus* and *Gordona* is 69.6% for sequencing of 16S rRNA and 89.3% for sequencing of *rpoB* gene. Sequencing of *rpoB* is useful for classification of mycobacteria due to its genetic diversity, but has some limitation in its application. In order to classify mycobacteria more accurately, it is important to combine sequencing of *rpoB* and 16S rRNA and biochemical/biological tests.

Key words：Identification of mycobacteria, 16S rRNA, Sequence, RIDOM, *rpoB* gene, Unidentified strain

Mycobacterium Reference Center, Research Institute of Tuberculosis, Japan Anti-Tuberculosis Association (JATA)

Correspondence to: Yuko Kazumi, TB Information Division (Molecular Epidemiology & Genetic Identification), Mycobacterium Reference Center, Research Institute of Tuberculosis, JATA, 3-1-24, Matsuyama, Kiyose-shi, Tokyo 204-8533 Japan. (E-mail：kazumi@jata.or.jp)

第81回総会シンポジウム

Ⅰ．結核分子疫学の新展開

座長 [1]高嶋 哲也 [2]岩本 朋忠

キーワーズ：結核分子疫学，IS*6110*RFLP，VNTR

シンポジスト：

1. 沖縄県での長期にわたるRFLP分析の成果と課題
   前田伸司（結核予防会結核研究所抗酸菌レファレンスセンター結核菌情報科）
2. VNTRの基礎とその応用
   西森 敬（動物衛生研究所ヨーネ病研究チーム）
3. VNTRの臨床応用とその成果
   松本智成，阿野裕美（大阪府立呼吸器・アレルギー医療センター臨床研究部）
4. 結核対策行政での分子疫学データの活用
   岩本朋忠（神戸市環境保健研究所微生物部）

特定菌株の追跡を可能とした分子技術である「結核菌遺伝子型別解析」は，従来からの疫学的手法と一体化することで，集団内での結核の分布を追及する科学，すなわち，結核分子疫学を生み出した。結核は空気感染で伝播し，感染から発病までに数カ月から数十年を要することから感染源や感染経路の特定がきわめて困難であったが，結核分子疫学の出現により，結核の疫学・対策・研究は新時代に突入したといえよう。

結核菌由来の挿入配列IS*6110*を用いたRestriction Fragment Length Polymorphism（RFLP）分析，いわゆるDNA指紋分析法による分子疫学的解析は，国内でも多くの施設で実施されており，特に集団感染事例での結核菌伝播の特定などに貢献している。また，解析対象を地域で分離された全菌株に拡大し，地域における感染実態の解明，結核対策プログラムの評価，未知の集団感染事例の発見などを目指し，結核対策改善に活用しようという動きもある。さらに，分子疫学データの臨床分野での応用も一部で既に実施されている。世界的な動きでは，施設間データ比較を可能とする迅速・簡便な遺伝子型別手法の開発ならびにグローバルデータベースの構築に向けた新たな取り組みが精力的になされており，地球規模での結核制圧に向け，結核分子疫学はますますその重要性を増してきているといえる。

本シンポジウムでは，わが国における分子疫学ネットワーク構築の一助となることを期待して，抗酸菌レファレンスセンター，基礎，臨床，行政の立場からの結核分子疫学の展望について，それぞれの分野に造詣の深い4人のシンポジストに概説していただいた。

前田伸司氏（結核予防会結核研究所抗酸菌レファレンスセンター）からは，沖縄県での約10年にわたるRFLP分析より得られた成果として，八重山における地域内流行型結核菌の存在と若年齢層でのクラスター形成率が高い傾向にあることが報告された。また，接触者調査の現場で分子疫学データをより有効に利用するには結果報告の迅速化や施設間でのデータ互換性が必要であることを強調された。西森敬氏（動物衛生研究所ヨーネ病研究チーム）には，IS*6110* RFLP法の欠点を補う新しい方法として期待されているVariable Numbers of Tandem Repeats（VNTR）法の基礎として，①VNTR領域発見の経緯，②VNTRの構造と多型形成のメカニズム，③系統発生的解析への応用に向けたアリルプロファイルの利用について概説いただいた。松本智成氏（大阪府立呼吸器・アレルギー医療センター臨床研究部）からは，VNTR法を医療現場に応用することにより，①多剤耐性結核は治療の失敗だけではなく感染発病していること，②内因性再燃および外来性再感染の区別が可能となること，③喀痰からの直接VNTRにより早期に薬剤耐性状況を推測できた事例，④*M. avium*症での再燃か再感染かの判断が可

[1]地方独立行政法人大阪府立病院機構大阪府立呼吸器・アレルギー医療センター，[2]神戸市環境保健研究所

連絡先：岩本朋忠，神戸市環境保健研究所，〒650-0046 兵庫県神戸市中央区港島中町4-6
(E-mail: tomotada_iwamoto@office.city.kobe.jp)
(Received 18 Jul. 2006)